THE ASTROPHYSICAL JOURNAL, 248:439–459, 1981 September 1


# THE STRUCTURE OF GIANT ELLIPTICAL GALAXIES IN POOR CLUSTERS OF GALAXIES

TRINH X. THUAN[1]
Astronomy Department, University of Virginia
AND
WILLIAM ROMANISHIN[2]
Astronomy Department, University of California, Los Angeles
*Received 1980 December 18; accepted 1981 March 18*

## ABSTRACT

Photographic surface photometry is presented for nine first brightest galaxies in poor clusters suspected to be cD galaxies by Morgan, Kayser, and White and by Albert, White, and Morgan. Exponentially truncated Hubble law and de Vaucouleurs $r^{1/4}$ law are fitted to the observed profiles to derive structural parameters. First brightest galaxies in poor clusters have profiles which are well fitted by an $r^{1/4}$ law over a range of more than 9 mag. They do not show the distinct envelope component seen in cD galaxies in rich clusters and in this sense are not "true" cD galaxies.

The structural parameters of first brightest galaxies in poor clusters are compared with those of cD galaxies in rich clusters and those of normal ellipticals. The central bodies (without the envelope in the case of rich clusters) of first brightest galaxies in both poor and rich clusters are similar to normal ellipticals except they are brighter and more diffuse (larger core and effective radii and lower surface brightness). The central parts of first brightest galaxies in poor clusters are more diffuse than those of cD galaxies in rich clusters and are about 0.6 mag brighter for a given cluster luminosity. The global ratio of mass to visual light derived for the first brightest galaxy in AWM 7 is $\sim 13$, similar to that seen in the central parts of cD galaxies and in normal ellipticals. The central parts of first brightest galaxies in poor and rich clusters are brighter by $\sim 1.1$ and $\sim 0.5$ mag, respectively, than the luminosity expected from a statistical formation process. A special creation process for first brightest cluster galaxies needs to be invoked.

The observations are consistent with the central body of first brightest galaxies being formed by about four mergers of galaxies with characteristic luminosity $L_*$ in rich clusters and about seven mergers in poor clusters, on the average, since cluster formation time. The faster merging rate in poor clusters is due to their compactness. The envelopes of cD galaxies in rich clusters are probably made of tidal debris from galaxy collisions. First brightest galaxies in poor clusters do not have an envelope because the collision time in these clusters is greater than the Hubble time.

*Subject headings:* galaxies: clusters of — galaxies: formation — galaxies: photometry — galaxies: structure

## I. INTRODUCTION

Supergiant cD galaxies have been the subject of many observational and theoretical studies in recent years. They are interesting objects because (1) they are used as "standard" candles in cosmological tests (Sandage, Kristian, and Westphal 1976; Hoessel, Gunn, and Thuan 1980) and (2) they may be the end product of dynamical evolution processes in clusters of galaxies such as galactic cannibalism (Hausman and Ostriker 1978) or tidal stripping in galaxy encounters (Richstone 1976) and thus serve as probes for studying these processes and measuring the degree of cluster dynamical evolution. This last datum is necessary if cD galaxies are to serve as useful cosmological probes. Much attention has been devoted to the study of supergiant cD galaxies in *rich* clusters since Matthews, Morgan, and Schmidt (1964) found that about one-half of all strong radio sources could be identified with these galaxies. Studies have been made of their dynamical properties (Dressler 1979) and their photometric structure (Oemler 1976; Hoessel 1980). A few years ago, Morgan, Kayser, and White (MKW) (1975) and Albert, White, and Morgan (AWM) (1977) published lists of about 20 *poor* clusterings which apparently contain supergiant cD galaxies. If these first brightest galaxies are genuine cD galaxies, they provide a unique opportunity to study cluster dynamical evolution in a very different environment from that in rich clusters of galaxies. To investigate the structure of these brightest galaxies in poor clusters, we have obtained deep photographic material for nine MKW and AWM clusters and

[1] Guest Investigator, Palomar Observatory, California Institute of Technology.

[2] Visiting Astronomer, Kitt Peak National Observatory, which is operated by the Association of Universities for Research in Astronomy, Inc., under contract with the National Science Foundation.

measured the light profile of the first brightest cluster member. In § II we describe the photographic surface photometry. In § III we discuss the relationship between the brightest galaxies in poor clusters, cD galaxies in rich clusters, and ordinary elliptical galaxies. In § IV we explore the implications of the data on theories of dynamical evolution in clusters of galaxies, and in § V we summarize our findings.

## II. PHOTOGRAPHIC SURFACE PHOTOMETRY

### *a) Plate Material*

We obtained for this investigation 10 sky-limited Palomar 48 inch (1.2 m) Schmidt plates. All the plates were in one of two bands: *g*, a band centered at 5000 Å and produced by a combination of a IIIa-J plate and a Wratten 4 filter, or *r*, a band centered at 6500 Å and produced by a combination of an 098 or IIIa-F plate and an RG 610 filter. The photometric system and its transformation to the *UBV* system are given in Thuan and Gunn (1976). Except for AWM 1 for which we had both *g* and *r* plates, all the other clusters (MKW 2, MKW 4, MKW 5, MKW 9, MKW 1s, AWM 4, AWM 5, and AWM 7) had only *g* or *r* material.

### *b) Plate Reduction*

All plates were scanned on the Kitt Peak National Observatory PDS microdensitometer. A 20 $\mu$m × 20 $\mu$m (1.″34 × 1.″34) aperture was used with a scanning step of 10 $\mu$m. The density to intensity transformation was done using the densities of the Gunn wedge exposed on each plate. The wedge had the property that the intensity varies linearly with distance along the wedge. A detailed description of the wedge can be found in Jensen and Thuan (1981). The densities $D$ measured at discrete "spots" on the wedge were then transformed to intensities $I$ using

$$\log I = a_0 + a_1 y + a_2 y^2 + a_3 y^3 , \qquad (1)$$

where $y = D + a_4 \log (1 - 10^{-D})$.

All picture processing operations made use of the Kitt Peak Interactive Picture Processing System (IPPS) described in Strom *et al.* (1977). The centers of the galaxies were found using the IPPS COMTAL display cursor. The axial ratio $b/a$ and position angle of each galaxy image as a function of radius are determined by setting the COMTAL cursor on the ends of the major and minor axes of different isophotes of the galaxy and by fitting an ellipse to each isophote. Only one galaxy (AWM 1) had a noticeable change of ellipticity with radius. For this galaxy, $b/a$ was 0.7 for $b < 12''$ and 0.85 for $b > 12''$.

The next step was to make a Fourier fit to the sky background variation as described in Strom and Strom (1978*a*). The sky intensity was sampled along a circle centered on the galaxy, but whose radius $R_0$ was several times larger than the galaxy's envelope. The resulting distribution along the circle was then fitted with a low-order Fourier series of the form $a_0 + f(\Phi)$. At any point $(r, \Phi)$ the background intensity was computed as $a_0 + r/R_0\, f(\Phi)$. This assumes that the background varies linearly along a ray drawn from the galaxy center through $(R_0, \Phi)$. This is a good assumption over domains where background variations are small, which is the case for the areas scanned on our plates. Then, intensities were measured in apertures of 2″ radius along elliptical paths characterized by $b$, the semiminor axis and whose axial ratio and position angle were determined as described before. The apertures were spaced to ensure that all the information in the picture was used, so that a much larger number of intensity values is sampled along the outer, as compared with the inner, isophotal contours. A point-rejection algorithm cleans each vector of points at a given $b$ of star images, other galaxies, and photographic defects; and a mean value of intensity was computed for that value of $b$. The intensities were sampled along paths with progressively larger values of $b$ until the sky was reached. The profile was followed far beyond the maximum detectable extent of the galaxy to ensure that the correct sky value was chosen. After the local sky value is chosen, the sky value is subtracted from the intensity at each $b$ and the profile $I(r)$ is displayed. The radius $r = (ab)^{1/2}$ is defined as the geometric mean of the semimajor and semiminor axes. In the outer parts of the profile, the intensities at several radii were averaged together to improve the ratio of signal to noise.

### *c) Photoelectric Calibration*

The profiles were then put on a magnitude scale using photoelectric photometry which was obtained for all the galaxies in the surface photometry program. We used photoelectric photometry in the *uvgr* system (Thuan and Gunn 1976) or *UBVR* photometry transformed to this system. The *uvgr* photometry was obtained with the Palomar 1.6 m telescope and the *UBVR* photometry with the Kitt Peak 1.3 m telescope. The aperture photometry is given in Table 1 both for galaxies whose surface photometry is presented in this paper and for other galaxies in the MKW and AWM lists.

The following equations were used to transform from *BVR* to *gr*:

$$g = V + 0.37(B-V) - 0.14 , \qquad (2)$$

$$r = R + 0.40(V-R) + 0.24 . \qquad (3)$$

Equation (2) is taken from Thuan and Gunn (1976), and equation (3) was derived using *r* measurements by Thuan and Gunn (1976) and *VR* measurements by Mendoza (1967) of Hyades stars. Additional *UBVR* photometry come from Schild and Davis (1979) (only their large-aperture photometry was used) and van den Bergh (1978). Several galaxies had photometry available from more than one of the above sources. The zero-points derived from comparing the photographic magnitudes to the various photoelectric magnitudes were in good agreement. The largest scatter in zero-point for a single galaxy was 0.1 mag, while the average scatter was about 0.05 mag. This intercomparison shows that any systematic error in our zero-points is at the 0.05 mag level or less. The calibrated profiles $\mu_g(r)$ and $\mu_r(r)$, where $r$ is in arcsec,

TABLE 1

PHOTOELECTRIC APERTURE PHOTOMETRY

| Cluster | Galaxy | $D$ (arcsec) | $V$ $g$ | $(B-V)$ $(v-g)$ | $(V-R)$ $(g-r)$ | $(U-B)$ $(u-v)$ |
|---|---|---|---|---|---|---|
| MKW 1[a] | NGC 3090 | 29.0 | 13.67 | 0.82 | 0.62 | 0.23 |
| | | 35.3[b] | 13.26 | 1.04 | 0.84 | |
| MKW 2 | 10276−0255 | 41.1 | 13.84 | 0.93 | 0.52 | 0.12 |
| MKW 3[a] | 11469−0311 | 41.1 | 14.81 | 0.16 | 0.19 | 0.00 |
| MKW 4 | NGC 4073 | 41.1 | 13.03 | 0.90 | 0.53 | 0.18 |
| MKW 5 | NGC 5400 | 41.1 | 13.86 | 0.88 | 0.58 | |
| MKW 9 | 15300+0451 | 35.3[b] | 14.41 | 1.05 | 0.96 | |
| MKW 10[a] | NGC 3825 | 41.1 | 13.48 | 0.74 | 0.50 | 0.20 |
| MKW 11[a] | NGC 5171 | 29.0 | 14.07 | ... | 0.50 | |
| MKW 12[a] | NGC 5724 | 41.1 | 13.73 | 0.70 | 0.55 | 0.18 |
| MKW 1s | 09175+0115 | 41.1 | 13.69 | 0.81 | 0.50 | 0.14 |
| MKW 2s[a] | 10246−0304 | 29.0 | 14.71 | 0.95 | 0.58 | 0.19 |
| MKW 4s[a] | NGC 4104 | 41.1 | 13.41 | ... | 0.53 | |
| AWM 1 | NGC 2804 | 29.0 | 13.96 | 0.94 | 0.55 | 0.17 |
| AWM 2[a] | NGC 4213 | 29.0 | 13.92 | 0.91 | 0.54 | 0.23 |
| AWM 3[a] | NGC 5629 | 17.7[b] | 13.50 | 1.01 | 0.84 | |
| | | 35.3[b] | 13.01 | 0.97 | 0.85 | |
| | | 41.1 | 13.18 | 0.75 | 0.48 | 0.24 |
| | | 58.6[b] | 12.72 | 0.97 | 0.84 | |
| AWM 4 | NGC 6051 | 17.7[b] | 14.30 | 1.15 | ... | |
| | | 29.0 | 14.16 | 1.04 | 0.62 | |
| | | 35.3[b] | 13.68 | 1.15 | ... | |
| | | 58.6[b] | 13.21 | 1.22 | ... | |
| AWM 5 | NGC 6269 | 17.7[b] | 13.94 | 1.14 | ... | |
| | | 29.0 | 13.82 | 1.03 | 0.61 | |
| | | 35.3 [b] | 13.38 | 1.14 | ... | |
| | | 58.6[b] | 13.05 | 1.08 | ... | |
| AWM 6[a] | IC 4062 | 29.0 | 14.06 | 1.01 | 0.55 | |
| AWM 7 | NGC 1129 | 35.3[b] | 13.11 | 1.19 | 0.97 | 0.70 |
| | | 58.6[b] | 12.42 | 1.15 | 0.94 | |

[a] Galaxies not having surface photometry.
[b] Apertures referring to *UBV* photometry. Apertures not marked refer to *uvgr* photometry.

are given in Table 2 for the MKW galaxies and in Table 3 for the AWM galaxies. The profiles of all nine galaxies plotted against $r^{1/4}$ (in units of $(\text{kpc})^{1/4}$) are given in Figure 1. To convert from arcsec to kpc we use redshift distances and a Hubble constant of 50 km $s^{-1}$ $Mpc^{-1}$. The redshifts are from Schild and Davis (1979), except that of NGC 1129 in AWM 7 which is taken from Schwartz *et al.* (1980).

### *d) Comparison with Other Authors and Accuracy of the Photometry*

One of the galaxies we observed, NGC 4073 in the cluster MKW 4, was also measured by Oemler (1976). Figure 2 shows a comparison of our surface photometry with that of Oemler. Our $g$ band was transformed to the $V$ band using equation (2). As Oemler did not have a good zero-point for this profile, we shifted his curve to obtain the best fit between the two profiles. The shift was 0.85 mag $\text{arcsec}^{-2}$ in the sense that Oemler's original profile was too faint. Oemler used the Zwicky *et al.* (1961–1968) magnitude to set the zero-point of his photographic photometry. Our work shows that Zwicky magnitudes for galaxies with diffuse envelopes are systematically too faint, as shown in Table 4 which compares our total apparent $B$ magnitudes $m_{B,\text{tot}}$ (obtained by integrating under the light profiles) to the Zwicky magnitudes $m_{\text{Zw}}$. The difference $m_{\text{Zw}} - m_{B,\text{tot}}$ grows larger as the galaxy becomes brighter in apparent magnitude, ranging from 0.8 mag at $m_{B,\text{tot}} = 14.5$ to 2.6 mag at $m_{B,\text{tot}} = 12.0$ for NGC 1129 in AWM 7 (Fig. 3). Evidently Zwicky's method of estimating apparent magnitudes is not sensitive to diffuse light components. The agreement with Oemler's profile is satisfactory, though not perfect. In the outer parts of the profile [$\log r(\text{kpc}) > 1.9$] our profile is systematically brighter than Oemler's. This is probably caused by a difference in the choice of the sky intensity. To bring our profile into rough agreement with Oemler's at large radii, we would have to increase our sky value by at least 3 times our estimated error in setting the sky value (about 0.2 mag at $\mu = 27$ mag $\text{arcsec}^{-2}$). Carter and Dixon (1978) also found in their study of M87 that Oemler's profile was fainter than theirs at large radii. They believed that Oemler might have overestimated the sky value by his two-dimensional polynomial sky fitting routine, which may fit not only to the variations in emulsion sensitivity but also to the low surface brightness outer regions of nearby objects. In the center of the MKW 4 profile, our photometry appears to be fainter than Oemler's. This is probably due to the very large photographic densities ($D > 5.1$) reached in this part of the galaxy

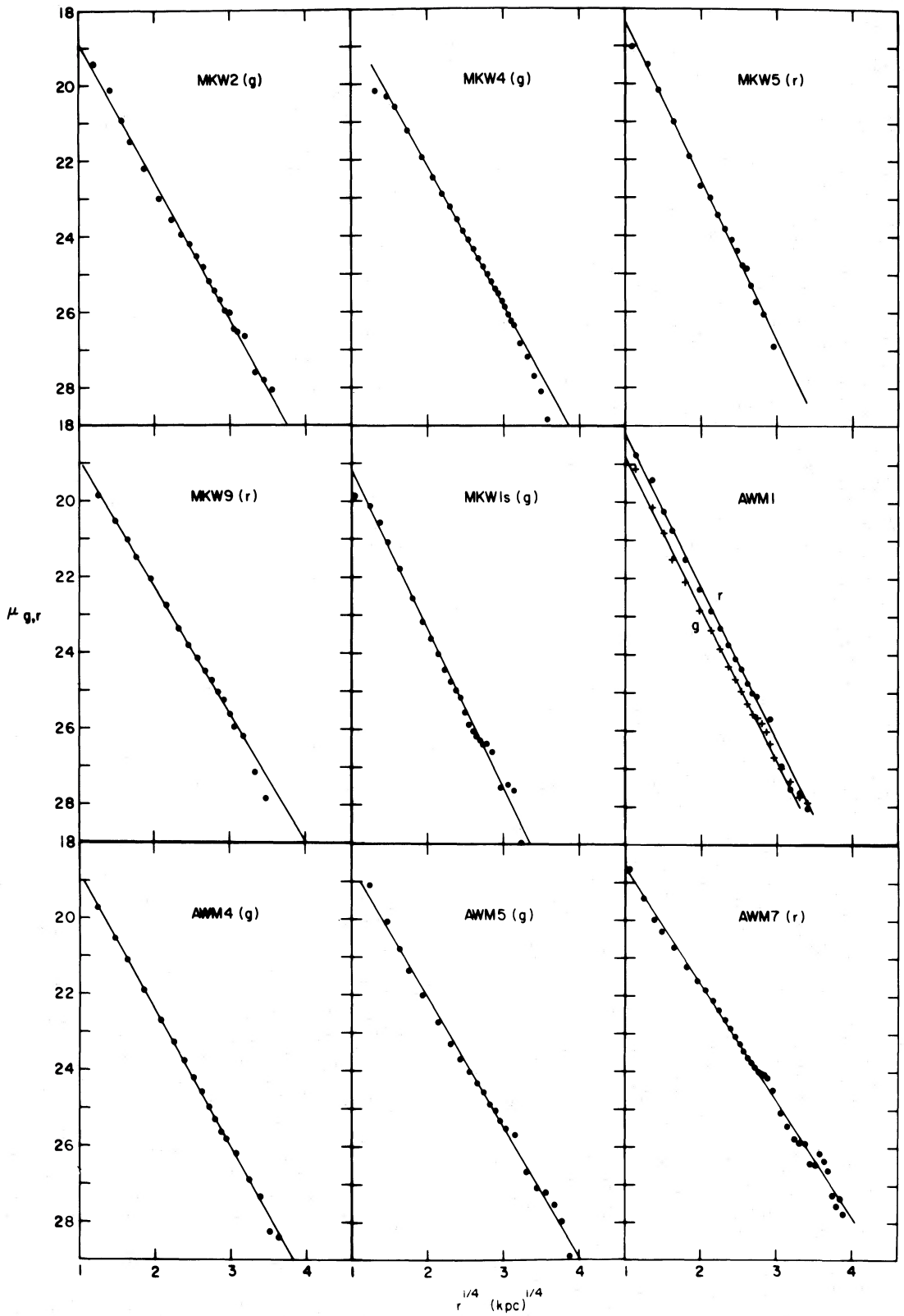


FIG. 1.—Profiles of the first brightest galaxies in nine poor clusters. The abscissa is $r^{1/4}$ in units of $(\mathrm{kpc})^{1/4}$. To convert from arcsec to kpc, redshifts from Schild and Davis (1979) and Schwartz *et al.* (1980) have been used with a Hubble constant of 50 km $s^{-1}$ $Mpc^{-1}$. The ordinate is the surface brightness in the *g* or *r* band (Thuan and Gunn 1976) in units of mag $arcsec^{-2}$. The solid lines are the de Vaucouleurs law (eq. [4]) fits to the data. The parameters of the fits are given in Table 6. The galaxy NGC 2904 in the cluster AWM 1 has both *g* and *r* profiles. There is no evidence of a color gradient in that galaxy.

TABLE 2

BRIGHTNESS PROFILES OF MKW GALAXIES

| MKW 2 | | MKW 4 | | MKW 5 | | MKW 9 | | MKW 1s | |
|---|---|---|---|---|---|---|---|---|---|
| $\sqrt{ab}$ | $\mu_g$ | $\sqrt{ab}$ | $\mu_g$ | $\sqrt{ab}$ | $\mu_r$ | $\sqrt{ab}$ | $\mu_r$ | $\sqrt{ab}$ | $\mu_g$ |
| 2.34 | 19.42 | 5.39 | 20.17 | 2.00 | 19.03 | 2.14 | 19.85 | 2.43 | 19.85 |
| 4.68 | 20.18 | 8.09 | 20.33 | 4.00 | 19.50 | 4.29 | 20.53 | 4.85 | 20.12 |
| 7.02 | 20.93 | 10.79 | 20.60 | 6.00 | 20.18 | 6.43 | 21.03 | 7.28 | 20.55 |
| 9.36 | 21.50 | 16.18 | 21.23 | 10.00 | 21.01 | 8.58 | 21.48 | 9.70 | 21.07 |
| 14.04 | 22.21 | 24.27 | 21.94 | 16.00 | 21.93 | 12.87 | 22.05 | 14.55 | 21.77 |
| 21.07 | 23.01 | 32.36 | 22.48 | 22.00 | 22.56 | 19.30 | 22.75 | 21.83 | 22.54 |
| 28.09 | 23.56 | 40.45 | 22.90 | 28.00 | 23.01 | 25.73 | 23.33 | 29.10 | 23.16 |
| 35.11 | 23.96 | 48.54 | 23.24 | 34.00 | 23.47 | 32.16 | 23.81 | 36.38 | 23.60 |
| 42.13 | 24.20 | 56.63 | 23.57 | 40.00 | 23.83 | 38.60 | 24.14 | 43.66 | 24.01 |
| 49.16 | 24.52 | 64.72 | 23.87 | 46.00 | 24.12 | 45.03 | 24.48 | 50.93 | 24.41 |
| 56.18 | 24.81 | 72.81 | 24.11 | 52.00 | 24.40 | 51.46 | 24.73 | 58.21 | 24.73 |
| 63.20 | 25.18 | 80.90 | 24.35 | 58.00 | 24.78 | 57.89 | 25.04 | 65.48 | 24.96 |
| 70.22 | 25.43 | 88.99 | 24.59 | 64.00 | 24.87 | 64.33 | 25.25 | 72.76 | 25.14 |
| 77.25 | 25.68 | 97.08 | 24.81 | 70.00 | 25.32 | 70.76 | 25.61 | 80.04 | 25.54 |
| 84.27 | 25.96 | 105.18 | 25.01 | 76.00 | 25.75 | 77.19 | 25.95 | 87.31 | 25.86 |
| 91.29 | 26.02 | 113.27 | 25.20 | 88.00 | 26.07 | 90.06 | 26.20 | 94.59 | 26.04 |
| 98.31 | 26.44 | 121.36 | 25.40 | 106.00 | 26.92 | 109.36 | 27.15 | 101.86 | 26.16 |
| 105.34 | 26.52 | 129.45 | 25.52 | | | 128.65 | 27.84 | 109.14 | 26.27 |
| 119.38 | 26.83 | 137.54 | 25.72 | | | 147.95 | 29.13 | 116.42 | 26.38 |
| 140.45 | 27.60 | 145.63 | 25.87 | | | | | 123.69 | 26.36 |
| 161.52 | 27.80 | 153.72 | 26.07 | | | | | 138.25 | 26.58 |
| 182.58 | 28.06 | 161.81 | 26.24 | | | | | 160.07 | 27.52 |
| | | 169.90 | 26.35 | | | | | 181.90 | 27.43 |
| | | 186.08 | 26.83 | | | | | 203.76 | 27.59 |
| | | 210.35 | 27.19 | | | | | 225.56 | 28.97 |
| | | 234.62 | 27.71 | | | | | | |
| | | 258.89 | 28.11 | | | | | | |
| | | 283.16 | 28.85 | | | | | | |

NOTE.—$\sqrt{ab}$ is in arcsec and $\mu$ is in magnitudes per square arcsec.

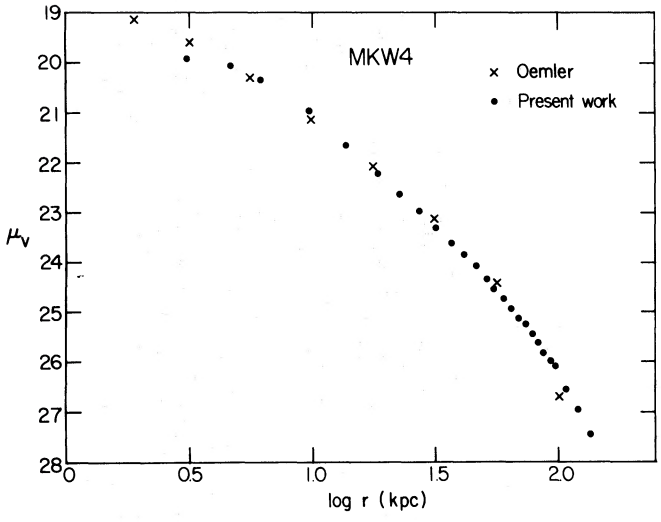


FIG. 2

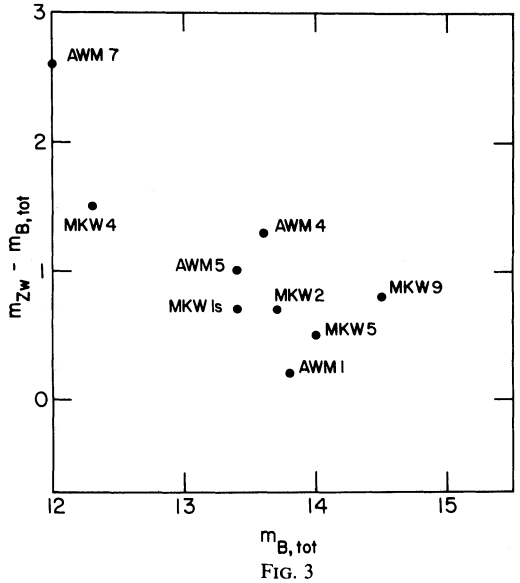


FIG. 3

FIG. 2.—Comparison of Oemler's (1976) profile of the galaxy NGC 4073 in the cluster MKW 4 with ours. Oemler's profile has been shifted upward by 0.85 mag arcsec$^{-2}$.

FIG. 3.—Comparison of Zwicky's (1961–1968) total apparent blue magnitudes $m_{Zw}$ with ours $m_{B,tot}$ obtained by integration of the light profiles. The difference $m_{Zw} - m_{B,tot}$ gets larger for galaxies with smaller apparent magnitude.

TABLE 3

BRIGHTNESS PROFILES OF AWM GALAXIES

| AWM 1 | | | AWM 4 | | AWM 5 | | AWM 7 | |
|---|---|---|---|---|---|---|---|---|
| $\sqrt{ab}$ | $\mu_g$ | $\mu_r$ | $\sqrt{ab}$ | $\mu_g$ | $\sqrt{ab}$ | $\mu_g$ | $\sqrt{ab}$ | $\mu_r$ |
| 2.17 | 19.12 | 18.75 | 2.56 | 19.72 | | | | |
| 4.34 | 20.12 | 19.39 | 5.12 | 20.54 | 2.31 | 19.09 | 2.31 | 18.66 |
| 6.51 | 20.80 | 20.23 | 7.68 | 21.10 | 4.62 | 20.06 | 4.62 | 19.43 |
| 8.68 | 21.49 | 20.73 | 12.80 | 21.89 | 6.93 | 20.78 | 6.93 | 19.99 |
| 13.02 | 22.08 | 21.50 | 20.49 | 22.69 | 9.24 | 21.36 | 9.24 | 20.31 |
| 19.52 | 22.83 | 22.28 | 28.17 | 23.27 | 13.86 | 22.02 | 13.86 | 20.73 |
| 26.03 | 23.35 | 22.85 | 35.85 | 23.75 | 20.78 | 22.73 | 20.78 | 21.24 |
| 32.54 | 23.84 | 23.31 | 43.53 | 24.20 | 27.71 | 23.30 | 27.71 | 21.60 |
| 39.05 | 24.29 | 23.74 | 51.21 | 24.57 | 34.64 | 23.71 | 34.64 | 21.84 |
| 45.56 | 24.64 | 24.10 | 58.90 | 24.97 | 41.57 | 24.04 | 41.57 | 22.13 |
| 52.06 | 24.95 | 24.37 | 66.58 | 25.29 | 48.50 | 24.34 | 48.50 | 22.37 |
| 58.57 | 25.28 | 24.75 | 74.26 | 25.63 | 55.43 | 24.57 | 55.43 | 22.63 |
| 65.08 | 25.56 | 25.01 | 81.94 | 25.81 | 62.35 | 24.89 | 62.35 | 22.86 |
| 71.59 | 25.65 | 25.09 | 97.31 | 26.19 | 69.28 | 25.06 | 69.28 | 23.07 |
| 78.09 | 25.79 | ... | 120.35 | 26.88 | 76.21 | 25.33 | 76.21 | 23.26 |
| 84.60 | 26.02 | ... | 143.40 | 27.33 | 83.14 | 25.53 | 83.14 | 23.46 |
| 91.11 | 26.33 | 25.68 | 166.45 | 28.25 | 96.99 | 25.69 | 90.07 | 23.64 |
| 97.62 | 26.69 | ... | 189.49 | 28.40 | 117.78 | 26.67 | 96.99 | 23.76 |
| 110.63 | 26.98 | 26.92 | | | 138.56 | 27.11 | 103.92 | 23.88 |
| 130.16 | 27.32 | 27.34 | | | 159.35 | 27.22 | 110.85 | 24.02 |
| 149.68 | 27.73 | 27.62 | | | 180.13 | 27.54 | 117.78 | 24.06 |
| 169.21 | 27.90 | 28.07 | | | 200.92 | 27.98 | 124.71 | 24.08 |
| 188.73 | 28.38 | | | | 221.70 | 28.89 | 131.64 | 24.17 |
| 208.25 | 29.25 | | | | | | 145.49 | 24.50 |
| | | | | | | | 166.28 | 25.11 |
| | | | | | | | 187.06 | 25.45 |
| | | | | | | | 207.85 | 25.78 |
| | | | | | | | 228.63 | 25.90 |
| | | | | | | | 249.42 | 25.91 |
| | | | | | | | 270.20 | 26.44 |
| | | | | | | | 290.98 | 26.48 |
| | | | | | | | 311.77 | 26.17 |
| | | | | | | | 332.55 | 26.37 |
| | | | | | | | 353.34 | 26.53 |
| | | | | | | | 374.12 | 27.29 |
| | | | | | | | 394.91 | 27.57 |
| | | | | | | | 415.69 | 27.37 |
| | | | | | | | 436.48 | 27.79 |

NOTE.—$\sqrt{ab}$ is in arcsec and $\mu$ is in magnitudes per square arcsec.

image on our plate. Fortunately, this was one of the worst plates in terms of the center being burnt out. In deriving the total magnitude for this galaxy (Table 4), we used a combination of photoelectric measurement (for the central region) and photographic measurement (for the rest of the galaxy).

TABLE 4

COMPARISON OF DERIVED TOTAL APPARENT BLUE MAGNITUDES WITH ZWICKY MAGNITUDES

| Cluster | $m_{Zw}$ | $m_{B,\,tot}$ | $m_{Zw} - m_{B,\,tot}$ |
|---|---|---|---|
| MKW 2 | 14.4 | 13.7 | 0.7 |
| MKW 4 | 13.8 | 12.3 | 1.5 |
| MKW 5 | 14.5 | 14.0 | 0.5 |
| MKW 9 | 15.3 | 14.5 | 0.8 |
| MKW 1s | 14.1 | 13.4 | 0.7 |
| AWM 1 | 14.0 | 13.8 | 0.2 |
| AWM 4 | 14.9 | 13.6 | 1.3 |
| AWM 5 | 14.4 | 13.4 | 1.0 |
| AWM 7 | 14.6 | 12.0 | 2.6 |

Stauffer and Spinrad (1980) have published recently a photometric profile of the galaxy NGC 1129 in the cluster AWM 7. Figure 4 compares their profile with ours. Because Stauffer and Spinrad did not have a zero-point, we have shifted their profile up by 0.70 mag arcsec$^{-2}$ so as to obtain the best agreement for the brighter parts of the profiles. Evidently the agreement in the outer parts of the galaxy ($\log r > 1.0$) is not very good. Stauffer and Spinrad's profile is already systematically fainter than ours at $\mu_r = 22$ mag arcsec$^{-2}$. Their photometry does not show the large envelope of NGC 1129. This may be due to their choice of a sky level in a region not totally free from the light of the low surface brightness envelope of the galaxy.

We next check Schild and Davis's (1979) photoelectric photometry against our photoelectric and photographic work. Schild and Davis have published small aperture (18".4 diameter) photometry of almost all the galaxies we

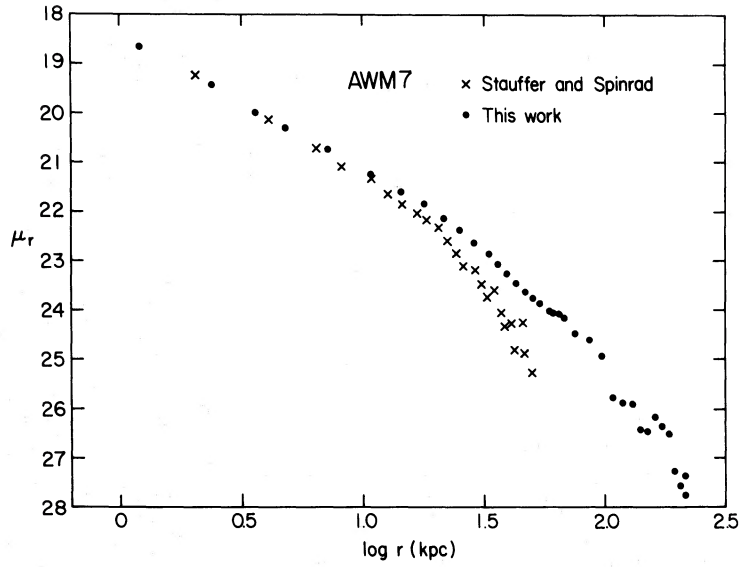


FIG. 4.—Comparison of the Stauffer and Spinrad (1980) profile of the galaxy NGC 1129 in the cluster AWM 7 with ours. Stauffer and Spinrad's profile has been shifted upward by 0.70 mag arcsec$^{-2}$.

observed. We measured the magnitudes in the same apertures on our plates, converted the photographic 18".4 diameter measurements to the $V$ passband and then compared with Schild and Davis's photoelectric photometry. Except for one galaxy, the agreement is very good, although we find our 18".4 diameter $V$ magnitudes systematically brighter than those of Schild and Davis by about 0.07 mag. We believe that this difference may be due to the uncertainty in the quoted sizes of the apertures used at the 1.6 m Mount Hopkins telescope. An overestimate of the aperture diameter by about 2" would account for the difference. Our photoelectric zero-point is probably more accurate: the three sets of photometry used were obtained with 3 different telescopes (the Palomar 1.6 m, the Kitt Peak 1.3 m, and the Cerro Tololo 1.3 m telescopes) and agree to better than 0.05 mag. The only large disagreement between Schild and Davis's small-aperture photometry and our calibrated photographic photometry within the same size aperture is for the first brightest galaxy in MKW 2 where our $V$ magnitude is 0.57 mag brighter than the Schild and Davis magnitude. Our calibration of the MKW 2 plate is reasonably certain, as we have two independent sources of photoelectric photometry, ours and that of van den Bergh (1978), which agree to better than 0.03 mag. The 0.07 mag shift does not account for the fact that our published total absolute visual magnitudes for the first brightest galaxies in poor clusters (Thuan and Romanishin 1980) are on the average about 0.8 mag brighter than that given by Schild and Davis. This discrepancy is due to two main sources as Table 5 shows: (1) Sandage's (1972*a*) mean growth curve for first-ranked ellipticals and radio galaxies, which was used by Schild and Davis (1979) in conjunction with their small-aperture photometry to derive a magnitude within the metric diameter of 86 kpc, is not appropriate for the brightest galaxies in poor clusters (see Fig. 5). Schild and Davis (1979) realized this fact. They obtained large-aperture photometry and derived a mean correction of 0.26 mag which they claim was applied to their visual magnitudes within the 86 kpc diameter $M_v$. A check of their $M_v$ reveals that this correction was not applied. This accounts for a mean difference of 0.39 ($\pm$0.17) mag (with MKW 2 excluded) between Schild and Davis's magnitudes and ours, as shown in column (6) of Table 5. (2) Schild and Davis's magnitudes measure the galaxy light within Sandage's (1972*a*) metric diameter of 86 kpc (corresponding to $\Delta$ mag = 0 in Fig. 5) while our magnitudes have been integrated over the entire galaxy. It is evident from Figure 5 that a nonnegligible amount of galaxy light is beyond the Sandage metric diameter. This accounts for a mean additional difference of 0.38 ($\pm$0.14) mag (col. [7] of Table 5), so that with the shift of 0.07 mag in the photoelectric zero-point, the difference of about 0.8 mag between Schild and Davis's total absolute visual magnitudes and ours is fully accounted for. We note that the $M_{V,\mathrm{tot}}$ given by Thuan and Romanishin (1980) are slightly different (by about 0.1 mag) from the ones given in column (5) of Table 5. This results from the use by Thuan and Romanishin (1979) of color transformation equations slightly different from the ones given by equations (2) and (3). The values of $M_{V,\mathrm{tot}}$ given here supersede the earlier ones.

We believe the accuracy of our photographic photometry to be better than 0.1 mag arcsec$^{-2}$ at surface brightnesses levels brighter than 25 mag arcsec$^{-2}$ in $g$, decreasing to several tenths of a magnitude arcsec$^{-2}$ at about 27 mag arcsec$^{-2}$. This decrease in accuracy is

TABLE 5

COMPARISON OF SCHILD AND DAVIS'S PHOTOMETRY WITH OURS

| Cluster (1) | $\theta_{Sand}$ (2) | $M_{V,Sand}$ (3) | $M_{V,SD}$ (4) | $M_{V,tot}$ (5) | $\Delta_1$ (6) | $\Delta_2$ (7) |
|---|---|---|---|---|---|---|
| MKW 2 ..... | 104″ | −23.37 | −22.51 | −23.76 | 0.86 | 0.39 |
| MKW 4 ..... | 156 | −23.53 | −23.06 | −23.96 | 0.47 | 0.43 |
| MKW 5 ..... | 125 | −22.82 | −22.62 | −22.98 | 0.20 | 0.16 |
| MKW 9 ..... | 83 | −23.14 | −22.52 | −23.57 | 0.62 | 0.43 |
| MKW 1s ..... | 184 | −22.61 | −22.26 | −22.83 | 0.35 | 0.22 |
| AWM 1..... | 114 | −23.15 | −22.99 | −23.43 | 0.16 | 0.28 |
| AWM 4..... | 100 | −23.51 | −22.92 | −23.95 | 0.59 | 0.44 |
| AWM 5..... | 91 | −23.82 | −23.51 | −24.36 | 0.31 | 0.54 |
| AWM 7..... | 170 | −23.90 | ... | −24.68 | ... | 0.56 |

NOTE.—Col. (2), $\theta_{Sand}$ is the angular diameter in arcsec corresponding to the Sandage (1972*a*) 86 kpc metric diameter. Col. (3), $M_{V,Sand}$ is the absolute visual magnitude within $\theta_{Sand}$ using photographic apparent magnitudes derived from the light profiles, *K*-corrections $K_V$ from Schild and Oke 1971, interstellar extinction corrections $A_V$ from Sandage 1973, redshifts from Schild and Davis 1979, and $H_0 = 50$ km s$^{-1}$ Mpc$^{-1}$. Col. (4), $M_{V,SD}$ is the absolute visual magnitude within $\theta_{Sand}$ from Schild and Davis 1979, with $K_V$ and $A_V$ as in col. (3). Col. (5), $M_{V,tot}$ is the total absolute visual magnitude obtained by integration of the light profile with $K_V$ and $A_V$ as in (3). Col. (6), $\Delta_1 = M_{V,SD} - M_{V,Sand}$. Col. (7), $\Delta_2 = M_{V,Sand} - M_{V,tot}$.

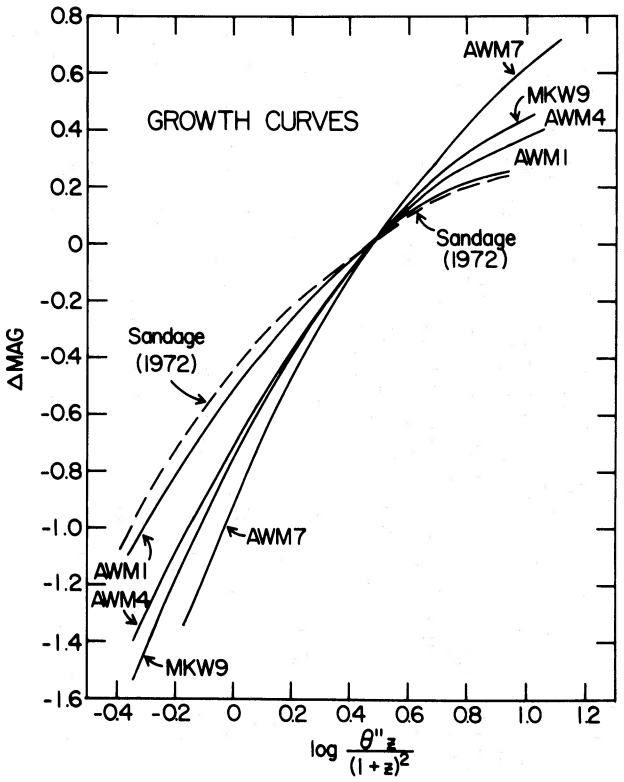


FIG. 5.—Growth of apparent magnitude with increasing measuring aperture of a few first brightest galaxies in poor clusters selected from this study (solid lines). For comparison, Sandage's (1972*a*) mean growth curve for first-ranked ellipticals and radio galaxies is given (*dashed curve*). Sandage's (1973) metric diameter of 86 kpc corresponds to Δ mag = 0.

mainly due to the uncertainty in the sky level, from statistics of the values of the intensities beyond the maximum extent of the galaxy.

## III. ANALYSIS

### *a) Fitting Functions*

In order to compare the structure of brightest galaxies in poor clusters with that of normal elliptical galaxies and that of cD galaxies in rich clusters, it is necessary to derive quantitative structural parameters for the studied galaxies. We have used for that purpose two fitting functions. One is the de Vaucouleurs (1948) law

$$\log I = \log I_e - 3.33\left[\left(\frac{r}{r_e}\right)^{1/4} - 1\right]. \quad (4)$$

Here $I$ is the surface brightness at radius $r$, $r_e$ is the effective radius containing half of the light of the model, and $I_e$ is the effective surface brightness at that radius. In magnitude units, $I_e$ corresponds to

$$B_e \equiv -2.5 \log I_e . \quad (5)$$

The second fitting function used is a Hubble law modified by an exponential cutoff as proposed by Oemler (1976):

$$I = \frac{I_0}{(1 + r/\beta)^2} \exp\left[-\left(\frac{r}{\alpha}\right)^2\right], \quad (6)$$

where $\beta$ is the core radius and $\alpha$ is the envelope exponential scale length. The exponential cutoff is needed to describe accurately the outer parts of elliptical galaxies. It is well known that Hubble's law, while accurately describing the central parts of ellipticals, breaks down at large radii where the galaxy surface brightness falls more

rapidly than an $r^{-2}$ power law. To characterize the inner part of the elliptical galaxy's profile which is well fitted by a power law, we shall use, following Oemler (1976), the reduced luminosity defined as:

$$L_{\rm rd} \equiv I_0 \beta^2 \,. \tag{7}$$

$M_{\rm rd}$ is the corresponding reduced magnitude:

$$M_{\rm rd} \equiv -2.5 \log L_{\rm rd} \,. \tag{8}$$

The reduced magnitude is independent of core and envelope size, as can be seen by rewriting equation (6) as

$$I = \frac{L_{\rm rd}}{(r+\beta)^2} \exp\left[-\left(\frac{r}{\alpha}\right)^2\right]. \tag{9}$$

It must be emphasized that the two fitting functions used here do not have a physical basis and serve the sole purpose of describing the light distribution in elliptical galaxies with a few parameters. Other simple empirical analytic functions or models having a more physical basis (such as the King 1966 models) can be used to fit spheroid profiles, but they convey essentially the same information (Kormendy 1977) and will not be discussed here. Standard nonlinear least-squares techniques were used to fit the functions (4) and (9) to the observed profiles of the first brightest galaxies in poor clusters. The results of the fitting are given in Table 6 for de Vaucouleurs's law and in Table 7 for Oemler's law. They are displayed graphically in Figures 1 and 6. In order to compare our results with that of Kormendy (1977) for normal ellipticals we have transformed the observed effective surface brightness $B_e$ to the $B$ system using the colors listed in Table 6, after correction for galactic interstellar extinction (Sandage 1973) and $K$-effects (Schild and Oke 1971). In Table 7, the reduced magnitude $M_{\rm rd}$ has been transformed to the $V$ system after interstellar extinction and $K$-corrections for comparison with Oemler's (1976) results for cD galaxies in rich clusters. The colors used are listed in Table 7. In deriving these colors, no attempt has been made to correct for aperture effects. We believe the aperture corrections to be small. The $g$ and $r$ profiles of the first brightest galaxy in AWM 1 are consistent with *no* color gradient down to a surface brightness level $\mu_g$ of about 26 mag arcsec$^{-2}$ (see Fig. 1).

TABLE 6

DE VAUCOULEURS PARAMETERS FOR BRIGHTEST GALAXIES IN POOR CLUSTERS

| Cluster | $A_B$ | $K_B$ | $B-g$ | $B-r$ | $B_{e,B}$[a] | log $r_e$[b] (kpc) |
|---|---|---|---|---|---|---|
| MKW 2 | 0.05 | 0.14 | 0.86 | 1.44 | 24.20 | 1.43 |
| MKW 4 | 0.00 | 0.10 | 0.81 | 1.36 | 23.85 | 1.42 |
| MKW 5 | 0.00 | 0.12 | 0.84 | 1.40 | 23.86 | 1.21 |
| MKW 9 | 0.05 | 0.18 | 0.80 | 1.32 | 25.00 | 1.59 |
| MKW 1s | 0.11 | 0.08 | 0.79 | 1.30 | 23.97 | 1.20 |
| AWM 1 | 0.07 | 0.13 | 0.80 | 1.30 | 23.67 | 1.27 |
| AWM 4 | 0.05 | 0.15 | 0.91 | 1.53 | 24.17 | 1.44 |
| AWM 5 | 0.09 | 0.17 | 0.82 | 1.36 | 24.08 | 1.54 |
| AWM 7 | 0.36 | 0.09 | 0.86 | 1.47 | 24.91 | 1.73 |

[a] Effective surface brightness in mag arcsec$^{-2}$ transformed to the $B$ system using eqs. (2) and (3) and corrected for galactic interstellar extinction $A_B$ (Sandage 1973) and including $K$-corrections $K_B$ (Schild and Oke 1971).

[b] $H_0 = 50$ km s$^{-1}$ Mpc$^{-1}$.

TABLE 7

OEMLER PARAMETERS FOR BRIGHTEST GALAXIES IN POOR CLUSTERS

| Cluster | $V_r$[a] (km s$^{-1}$) | $g-V$ | $V-r$ | $M_{V,\rm rd}$ | log $\alpha$ (kpc) | log $\beta$ (kpc) | log $R_1$ (kpc) | $L_{V,\rm cl}$[b] ($10^{11}\,L_\odot$) |
|---|---|---|---|---|---|---|---|---|
| MKW 2 | 8960 | 0.28 | 0.30 | −20.62 | 2.26 | 0.32 | 2.32 | 1.61 |
| MKW 4 | 5869 | 0.25 | 0.30 | −21.18 | 2.08 | 0.62 | 2.22 | 2.08 |
| MKW 5 | 7404 | 0.27 | 0.29 | −20.15 | 1.85 | 0.32 | 1.96 | 0.94 |
| MKW 9 | 11467 | 0.25 | 0.27 | −20.85 | 2.07 | 0.73 | 2.23 | 2.32 |
| MKW 1s | 4938 | 0.24 | 0.27 | −19.69 | 2.03 | 0.22 | 2.06 | 0.30 |
| AWM 1 | 8150 | 0.24 | 0.26 | −20.22 | 2.06 | 0.16 | 2.22 | 1.87 |
| AWM 4 | 9381 | 0.31 | 0.31 | −20.95 | 2.20 | 0.50 | 2.24 | 1.40 |
| AWM 5 | 10350 | 0.26 | 0.28 | −21.20 | 2.36 | 0.43 | 2.37 | 5.63 |
| AWM 7 | 5250 | 0.29 | 0.32 | −21.32 | 2.41 | 0.77 | >2.60 | 1.60 |

[a] The redshifts are from Schild and Davis 1979, except that of AWM 7 which is from Schwartz *et al.* 1980.

[b] $B-V = 1.0$ has been adopted.

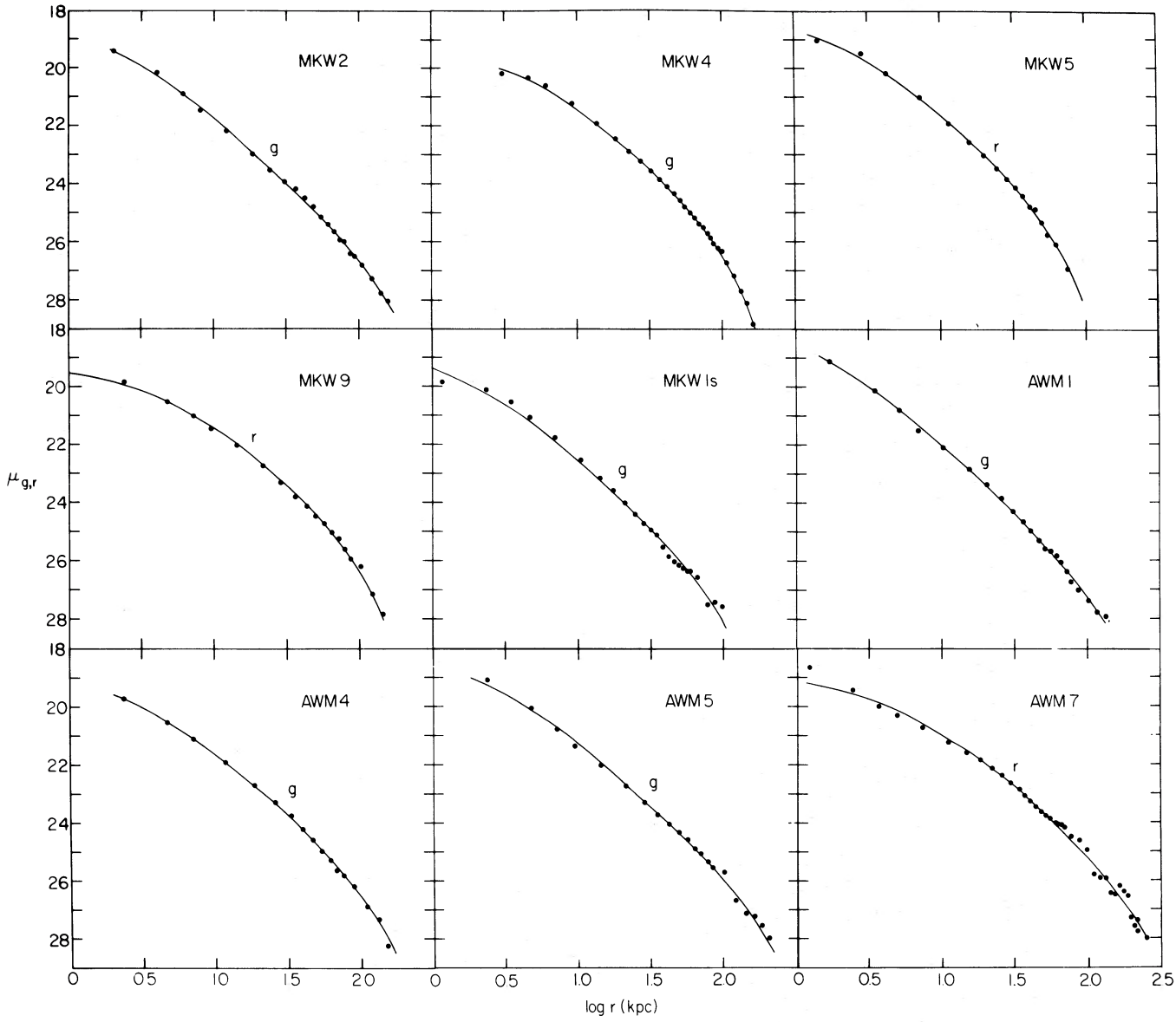


FIG. 6.—Profiles of the first brightest galaxies in nine poor clusters. Surface brightness in $g$ or $r$ (Thuan and Gunn 1976) in units of mag arcsec$^{-2}$ is plotted against the log of the radius in kpc. Redshifts are from Schild and Davis (1979) and Schwartz *et al.* (1980), and a Hubble constant of 50 km s$^{-1}$ Mpc$^{-1}$ is used. The solid lines are truncated Hubble law (eq. [6]) fits to the data. The parameters of the fits are given in Table 7. The fits are generally very good except for the inner regions of the brightest galaxies in MKW 1s and AWM 7.

The fit is in general very good (the $\chi^2$ for the fit is of order unity per degree of freedom), as can be seen from Figures 1 and 6, although de Vaucouleurs's law appears to provide a better fit for the inner regions of certain galaxies, e.g., the first brightest galaxies in MKW 1s and AWM 7. The core radii $\beta$ listed in Table 7 (and in Table 3 of Oemler's 1976 paper) have not been corrected for seeing effects. The true core radius may be 1.1 to 2 times smaller. The $\beta$'s should be considered here simply as parameters defining the fit of a truncated Hubble law to the observed profiles. In the following discussion which involves correlations between physical structural parameters (§ III*b*), we shall not make use of $\beta$. Also listed in Table 7 are the cutoff radius $R_1$ for each galaxy determined by visually estimating the radius where the brightness profile drops to zero.

Oemler (1976) gives structural parameters for the truncated Hubble law in his study of cD galaxies in rich clusters. In order to compare with the de Vaucouleurs parameters derived for the brightest galaxies in poor

clusters we have fitted the inner regions of the cD galaxies studied by Oemler with de Vaucouleurs's law. The results are given in Table 8 and the fits are displayed graphically in Figure 7.

### b) *Comparison of Brightest Galaxies in Poor Clusters with Normal Ellipticals and cD Galaxies in Rich Clusters*

How do the first brightest galaxies in the poor clusters, which on photographic plates look very much like cD galaxies, fit in the sequence of spheroidal galaxies from normal average luminosity elliptical galaxies to luminous cD galaxies in rich clusters with large extended envelopes? The answer to this question may well provide clues to the formation process of ellipticals and cD galaxies. We use the data of Kormendy (1977) and Oemler (1976) for elliptical galaxies and that of Oemler (1976) for cD galaxies in rich clusters to compare to our own. One of the main themes and conclusions to be developed in the following sections is already apparent from a comparison of Figures 1 and 7. The profiles of the brightest galaxies in poor clusters are very well fitted by a de Vaucouleurs law over a range of more than 9 mag in brightness. By contrast there is a substantial excess of light above the de Vaucouleurs law in the outer regions of *all* cD galaxies in rich clusters studied by Oemler (1976). Evidently *the cD galaxies in rich clusters possess an extra component of stellar light which is not present in brightest galaxies in poor clusters. This extra component of light constitutes the major difference between first brightest galaxies in poor and rich clusters.* To emphasize this difference, we shall consider, in our comparison of the structural properties of normal ellipticals with that of brightest galaxies in poor and rich clusters, not only correlations between parameters which exclude the extra component of light but also between those which include it.

Figures 8 and 9 show the correlation between the absolute visual reduced magnitude $M_{V,\mathrm{rd}}$ of first brightest galaxies in poor and rich clusters (a parameter which describes only the inner region of each galaxy and thus exclude the envelope) and their cutoff radius $R_1$ and their total absolute visual magnitudes. These last two parameters describe the whole galaxy and thus include the envelope. There is a striking difference between the brightest galaxies in poor clusters and those in rich clusters. The brightest galaxies in poor clusters clearly fall along the brightward extrapolation of the $(M_{V,\mathrm{tot}}, M_{V,\mathrm{rd}})$ and $(\log R_1, M_{V,\mathrm{rd}})$ relation for normal ellipticals ($M_{V,\mathrm{rd}} \gtrsim -20$) derived by Oemler (1976):

$$M_{V,\mathrm{tot}} = -7.36 + 0.79 M_{V,\mathrm{rd}}, \quad (10)$$

$$\log R_1(\mathrm{kpc}) = -3.20 - 0.26 M_{V,\mathrm{rd}}. \quad (11)$$

The dispersion of the poor cluster points about the $(\log R_1, M_{V,\mathrm{rd}})$ line is only 0.17 in $\log R_1$(kpc), and that about the $(M_{V,\mathrm{tot}}, M_{V,\mathrm{rd}})$ line only 0.20 mag. In contrast, all the cD galaxies in rich clusters studied by Oemler (1976) deviate systematically from the normal elliptical line: they consistently have a larger $R_1$ and $M_{V,\mathrm{tot}}$ for their reduced magnitude, as compared to normal ellipticals (the large cD galaxies in A2670 and A1413 being the extreme cases). Another point is clear from Figures 8 and 9: the brightest galaxies in poor and rich clusters cannot be distinguished on the basis of their reduced magnitudes (which characterize only the inner parts of the galaxies) alone: the range of their $M_{V,\mathrm{rd}}$ overlap almost exactly from about $-19.5$, the bright end of normal ellipticals, to about $-21.5$.

We next look at the relation between two structural quantities which both describe only the inner regions of the first brightest galaxies: the de Vaucouleurs effective blue surface brightness $B_{e,B}$ and radius $r_e$. Kormendy (1977, 1980) has established that normal ellipticals define a tight linear relationship in the $(B_{e,B}, \log r_e)$-plane:

$$B_{e,B} = 3.28 \log r_e(\mathrm{kpc}) + 19.45 \text{ mag arcsec}^{-2}, \quad (12)$$

with a dispersion of only 0.38 $B$ mag arcsec$^{-2}$. Equation

TABLE 8

DE VAUCOULEURS PARAMETERS FOR OEMLER'S cD GALAXIES IN RICH CLUSTERS

| Cluster | Galaxy | $V_r$[a] (km s$^{-1}$) | $B-V$ | $A_B$ | $K_B$ | $B_{e,B}$[b] | $\log r_e$[c] (kpc) |
|---|---|---|---|---|---|---|---|
| Perseus | NGC 1275 | 5486 | 0.76[d] | 0.44 | 0.09 | 22.28 | 1.21 |
| Virgo | M87 | 1020 | 0.94[d] | 0.00 | 0.02 | 22.59 | 1.00 |
| A779 | NGC 2832 | 5996 | 1.00[d] | 0.06 | 0.10 | 22.19 | 0.904 |
| A1413 | ... | 42780 | 1.00 | 0.00 | 0.71 | 23.15 | 1.50 |
| A2147 | 1600.0+1606 | 11302 | 1.00 | 0.06 | 0.18 | 24.28 | 1.43 |
| A2162 | NGC 6086 | 9533 | 1.00 | 0.05 | 0.15 | 21.79 | 0.820 |
| A2199 | NGC 6166 | 9353 | 1.06[d] | 0.06 | 0.15 | 23.02 | 1.30 |
| A2670 | ... | 23220 | 1.00 | 0.00 | 0.38 | 23.31 | 1.37 |

[a] The redshifts are from Noonan 1973, except that of Virgo which is from Aaronson *et al.* 1980.

[b] Effective surface brightness in mag arcsec$^{-2}$ transformed to the $B$ system using eqs. (2) and (3) and corrected for galactic interstellar extinction $A_B$ (Sandage 1973) and including $K$-corrections $K_B$ (Schild and Oke 1971).

[c] $H_0 = 50$ km s$^{-1}$ Mpc$^{-1}$.

[d] From the Second Reference Catalogue (de Vaucouleurs, de Vaucouleurs, and Corwin 1976). $(B-V) = 1.0$ has been adopted for galaxies not possessing color measurements.

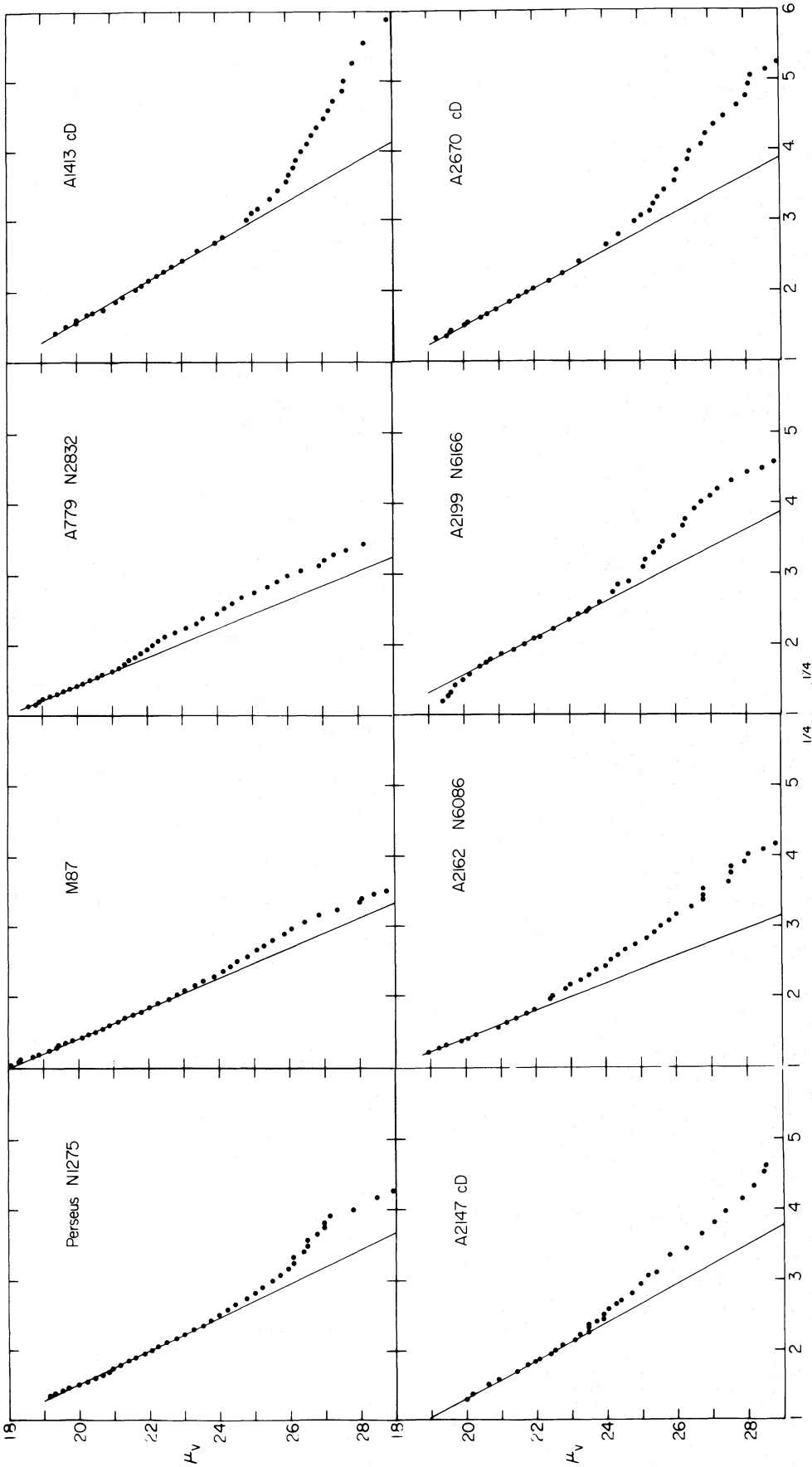


FIG. 7.—Profiles of cD galaxies in eight rich clusters studied by Oemler (1976). Visual surface brightness in mag arcsec$^{-2}$ is plotted against $r^{1/4}$ in units of (kpc)$^{1/4}$. The redshifts are from Noonan (1973), and a Hubble constant of 50 km s$^{-1}$ Mpc$^{-1}$ is adopted. The inner region of each cD galaxy has been fitted to de Vaucouleurs's law (*solid line*). The parameters of the fits are given in Table 8.

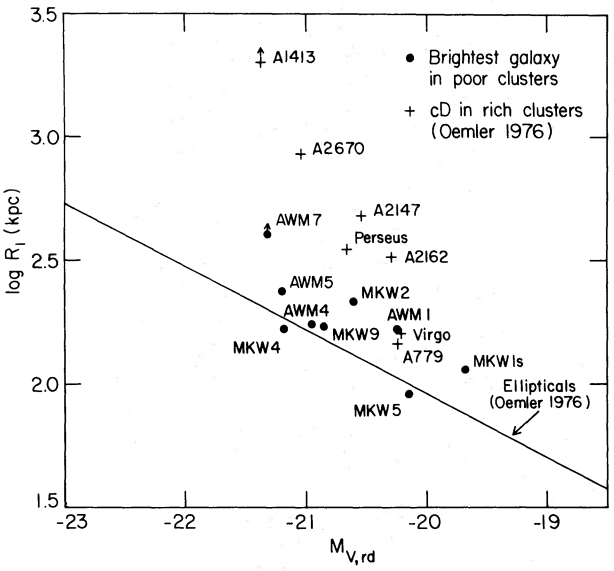


FIG. 8.—The logarithm of the visually estimated limiting radii $R_1$ (in kpc) of brightest galaxies in poor and rich clusters versus their absolute visual reduced magnitudes. The solid line is the relation derived by Oemler (1976) for normal ellipticals (eq. [11] in text).

(12) is represented by the solid line in Figure 10. It is apparent from this figure that the brightest galaxies in *both* poor and rich clusters follow well the brightward extrapolation of the relation (12) defined by normal ellipticals. The brightest galaxies in the poor clusters appear to scatter randomly about the mean line and have a dispersion of only 0.24 $B$ mag arcsec$^{-2}$. The brightest galaxies in the rich clusters also clearly follow relation (12), although, with the exception of A2147, they lie

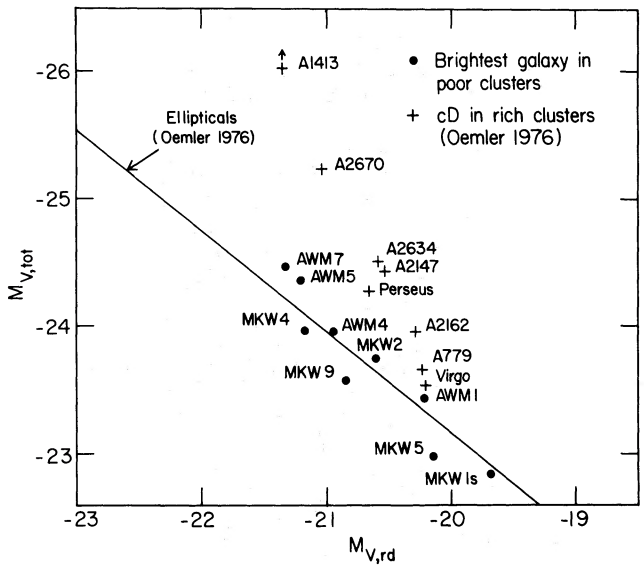


FIG. 9.—The relation between reduced and total magnitudes of brightest galaxies in poor and rich clusters. The total magnitudes have been derived by integrating the light profile. The solid line represents the relation derived by Oemler (1976) for normal ellipticals with $M_{V,\mathrm{rd}} < -19.2$ (eq. [10] in text).

systematically above the mean line defined by normal ellipticals, having brighter effective surface brightness for their effective radius. The dispersion is larger, being 0.76 $B$ mag arcsec$^{-2}$. The magnitude of the deviation from the mean line appears to be uncorrelated with the amount of light in the envelope of the galaxy. N1275 in the Perseus cluster, which has a relatively small envelope (Fig. 7), has a surface brightness 1.14 mag arcsec$^{-2}$ brighter than a normal elliptical with the same effective radius, while the extreme cD galaxy in 2670 with a much more extended envelope deviates only by 0.62 $B$ mag arcsec$^{-2}$ from the mean line. The extreme cD galaxy in A1413 with the most luminous envelope of the galaxies in the sample also deviates the most from the mean line (1.30 $B$ mag arcsec$^{-2}$). In general, however, all brightest galaxies follow the mean line whether they are in rich or in poor clusters. The best fit to all cluster points is steeper than the solid line in Figure 10, but not significantly so. The dispersion for all galaxies is 0.57 $B$ mag arcsec$^{-2}$, only slightly larger than that obtained by Kormendy (1977) for normal ellipticals.

The existence of a tight ($B_{e,B}$, log $r_e$)-relationship for the brightest galaxies in poor and rich clusters suggests that each parameter may correlate individually with the absolute magnitude (or luminosity) of the galaxy. Again we must be careful to choose an absolute magnitude which describes only the inner regions of the galaxy. The use of any magnitude which includes the contribution of the envelope luminosity will wash out the correlations. We use here the visual absolute reduced magnitude $M_{V,\mathrm{rd}}$. Figures 11 and 12 show $B_{e,B}$ and $r_e$ of brightest galaxies in poor and rich clusters plotted against $M_{V,\mathrm{rd}}$. Although the scatter is large, the correlations are present. Brighter galaxies are on the average more diffuse: they have lower effective surface brightness and larger effective radii. These relationships are well known to hold for normal ellipticals. Using the (log $r_e$, $M_{V,\mathrm{tot}}$)-relation, with $r_e$ measured on $U$ plates and for E and S0 galaxies in the Coma cluster center as given by Strom and Strom (1978*a*), and equation (10), we derive the following relation for normal ellipticals:

$$\log r_e(\mathrm{kpc}) = -3.09 - 0.20 M_{V,\mathrm{rd}} \,. \qquad (13)$$

Equation (13) is represented by the solid line in Figure 12. It is evident that, although the less bright galaxies (like the first brightest galaxies in the Virgo, A779, and A2162 clusters) follow well the brightward extrapolation of equation (13), the first brightest galaxies in *both* poor and rich clusters have systematically a larger effective radius for their absolute reduced magnitude as compared with normal ellipticals; i.e., the (log $r_e$, $M_{V,\mathrm{rd}}$)-relation turns upward for the brightest galaxies. Equation (13) changes slightly, depending (weakly) on the color of the plate on which $r_e$ is measured, and (strongly) on the location of the galaxies measured. Strom and Strom (1978*a*, *b*) found that galaxies in high-density environments (such as in cluster cores or in dense clusters of galaxies) have smaller $r_e$ for a given $M_{V,\mathrm{rd}}$ than galaxies in less dense environments. They attribute this effect to tidal stripping of the

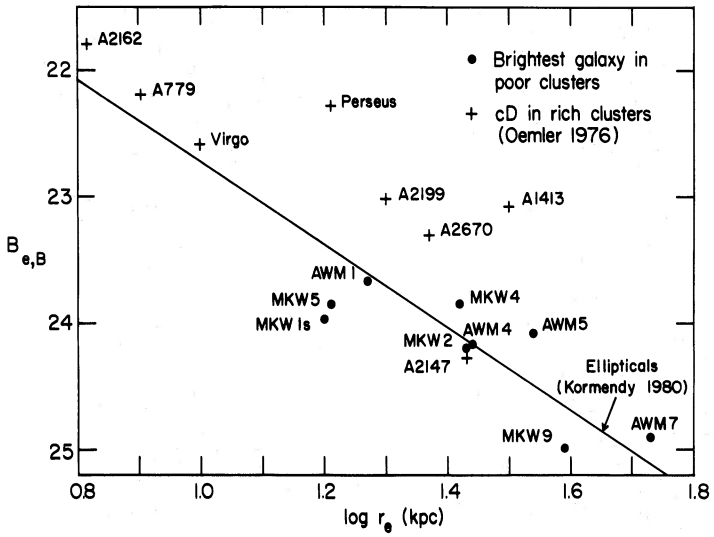


FIG. 10.—The de Vaucouleurs blue effective surface brightness versus the logarithm of the effective radius (in kpc) for first brightest galaxies in poor and rich clusters. The solid line is the relation derived by Kormendy (1980) for normal ellipticals (eq. [12] in text).

outer regions of galaxies in galaxy-galaxy collisions. These environmental effects shift the solid line in Figure 12 up or down slightly (at most by 0.2 in log $r_e$) while maintaining nearly the same slope (Strom and Strom 1978*a*, *b*), but do not change qualitatively our remarks concerning the larger size of $r_e$ of first brightest galaxies in poor and rich clusters. Since the latter follow well the brightward extrapolation of the ($B_e$, log $r_e$)-relation for ellipticals, one must conclude that the first brightest galaxies in poor and rich clusters also have a *lower* effective surface brightness at a given reduced absolute magnitude as compared to normal ellipticals.

Another point is evident from Figures 11 and 12. Although there is some slight overlap (such as the brightest galaxy in A2147), the first brightest galaxies in poor clusters are in general more diffuse (smaller effective surface brightness and larger effective radii) than the cD galaxies in rich clusters.

### c) *Relationship of First Brightest Galaxies with Cluster Luminosities*

To gain insight into the formation processes of first brightest galaxies, it is useful to investigate possible

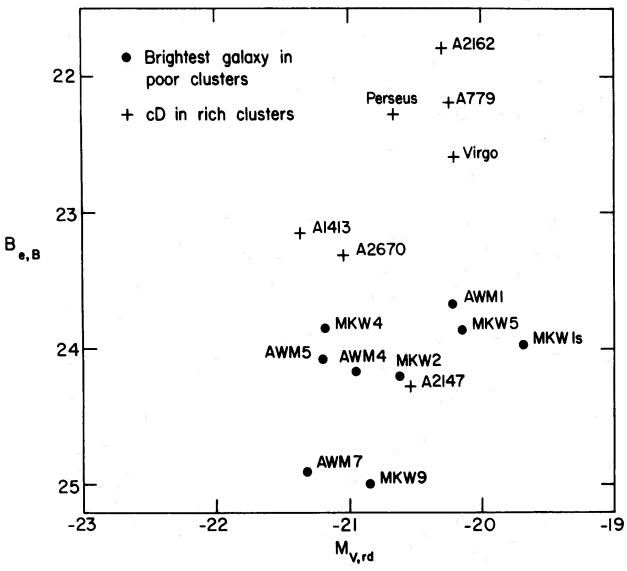


FIG. 11

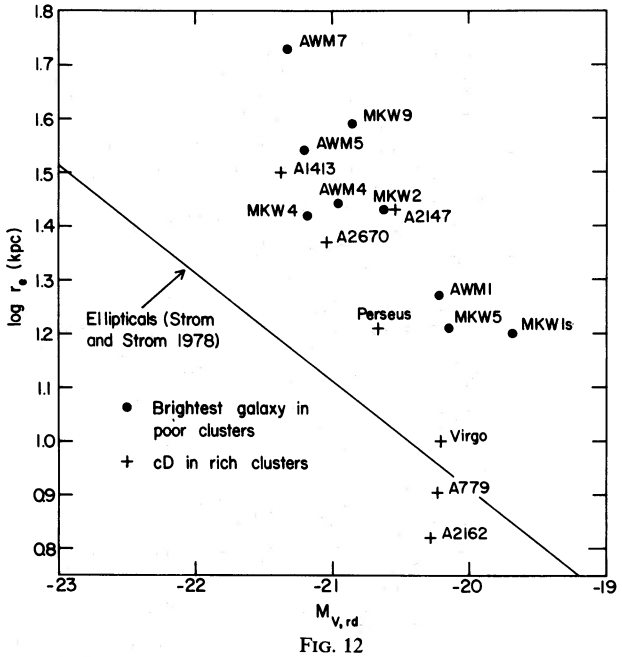


FIG. 12

FIG. 11.—The de Vaucoulers blue surface brightness versus the absolute visual reduced magnitude of brightest galaxies in poor and rich clusters.
FIG. 12.—The de Vaucoulers effective radius versus the absolute visual reduced magnitude of brightest galaxies in poor and rich clusters. The solid line is the relation derived for normal ellipticals by Strom and Strom (1978*a*).

correlations between properties of individual first brightest galaxies and global properties of the clusters in which they are located. In particular, the cluster luminosity is a useful datum: if first brightest galaxies are made by mergers of other galaxies, it is a measure of available visible material in the cluster.

To calculate the luminosity of the poor clusters, we estimate first the total brightness of those cluster members listed by Zwicky *et al.* (1961–1968) within a circle of diameter of about 1 Mpc centered on the first brightest galaxy. We used our derived magnitudes for the first brightest galaxies (Table 4) and Zwicky magnitudes for the other galaxies. In contrast to our finding that Zwicky magnitudes underestimate the true luminosity of large galaxies with diffuse outer parts (§ II*d*), Huchra (1976) has shown that, for normal galaxies, Zwicky magnitudes are reliable except for a scale shift of 0.36 mag with respect to Holmberg's (1958) *B* scale, in the sense that Zwicky magnitudes are fainter. We convert the Zwicky magnitudes to Holmberg's *B*-magnitudes which approximate better total magnitudes. The diameter of 1 Mpc of the circle within which galaxies are assumed to belong to the cluster is only approximate. All poor clusters were examined on the Palomar Sky Survey prints and on the Zwicky *et al.* (1961–1968) charts, and all galaxies which appear to belong to the surface density enhancement formed by the poor cluster were included. Redshift data on individual cluster members of the poor clusters to establish membership is still scarce. Nevertheless, redshift measurements of suspected galaxies in the poor clusters MKW 4 and MKW 1s (as marked on the finding charts given in MKW and AWM) by Thomas and Batchelor (1978), and in AWM 1, AWM 5, and AWM 7 by Stauffer and Spinrad (1980), all confirm the true membership of these galaxies. In only one case, that of AWM 4, did the redshift measurements (Stauffer and Spinrad 1978) reveal some galaxies (Nos. 3 and 5 in the finding chart of AWM) which were not members. The remaining galaxies (Nos. 1, 2, and 4) are true members. We have measured the redshift of galaxy No. 6 [$v_r$ (heliocentric) = 9358 km s$^{-1}$] which is also a true member. Thus we feel that our assignment of galaxy membership is reasonably accurate. The 1 Mpc diameter adopted is somewhat smaller than the usual sizes quoted for clusters of galaxies; but as Bahcall (1980) has also noticed, the poor clusters appear to have core radii a factor of 2 or so smaller than richer clusters of galaxies.

We next correct for the light contribution from galaxies fainter than $m_{Zw} = 15.7$. We use the luminosity function proposed by Schechter (1976) with the parameters found by Turner and Gott (1976) for small groups of galaxies:

$$N(L)dL = N^*(L/L^*)^{-1} \exp(-L/L^*)dL\,, \qquad (14)$$

where $N^*$ is a constant measuring cluster richness and $L_{Zw}{}^* = 3.4 \times 10^{10}\ L_\odot$. The ratio of the total luminosity of the poor cluster to that observed in galaxies with $m_{Zw} < 15.7$ is

$$\frac{L_{tot}}{L_{obs}} = \exp\left(\frac{d}{d^*}\right)^2, \qquad (15)$$

where $d$ is the distance to the cluster and $d^* = 204$ Mpc is the distance at which a galaxy with luminosity $L^*$ has an apparent magnitude of 15.7. The correction factor given in equation (15) ranges from 1.3 to 2.3 for all clusters, except for AWM 5 and MKW 9 which have correction factors of 2.8 and 3.5, respectively. These correction factors may be too large and should be regarded as upper limits, especially because the poor clusters appear to lack in faint members. A detailed study of the luminosity function of galaxies in the poor clusters to check equation (14) would be valuable. Work on this topic (Thuan 1981) using our deep photographic material is in progress, although no firm results are available as yet. Finally we convert the cluster blue luminosity to a visual luminosity in order to compare with Oemler's (1976) total visual luminosities for rich clusters, using $(B-V) = 1.0$. The poor cluster luminosities are given in Table 7.

The relation between total galaxy absolute magnitude (as given in Table 5) and total cluster luminosity is plotted in the upper half of Figure 13. The poor cluster luminosities represent a smooth extension of the rich cluster luminosities. This is in agreement with the study made by Bahcall (1980), who also found that the MKW–AWM clusters represent a smooth continuation of the characteristics (such as richness, galaxy surface densities, and spiral galaxy fractions) of the rich Abell clusters. Oemler (1976) already remarked on the strong dependence of the first brightest galaxy luminosity $L_{gal}$ on the total luminosity of the rich clusters $L_{cl}$: $L_{gal} \sim L_{cl}{}^{1.25}$. Our data show that this strong dependence does not continue at lower cluster

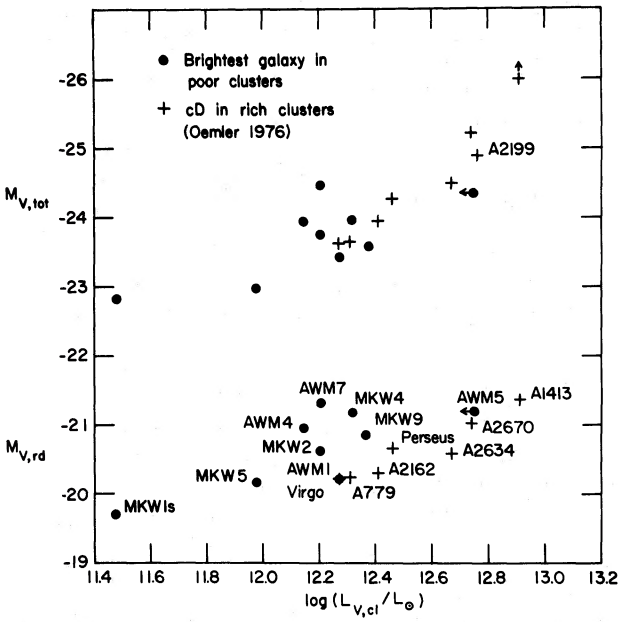


FIG. 13.—The upper half of the figure shows the total visual absolute magnitude of the first brightest galaxy in poor and rich clusters versus the visual luminosity $L_{V,cl}$ of their clusters. The total magnitudes are obtained by integrating the light profiles. The bottom half of the figure shows the reduced visual absolute magnitude of the first brightest galaxy in poor and rich clusters versus the visual luminosity of their clusters.

luminosities. The relation $M_{V,\mathrm{tot}}$–$L_{V,\mathrm{cl}}$ flattens out considerably for $L_{V,\mathrm{cl}} < 2 \times 10^{12}\ L_{V\odot}$ ($L_{\mathrm{gal}} \sim L_{\mathrm{cl}}^{0.36}$), although clusters with larger luminosities still have brighter first brightest galaxies.

The lower half of Figure 13 shows the correlation between the envelope-independent reduced visual absolute magnitude of first brightest galaxies and the total visual cluster luminosity. The first brightest galaxies in the poor clusters extend smoothly the correlation $M_{V,\mathrm{rd}}$–$L_{V,\mathrm{cl}}$ exhibited by the cD galaxies in rich clusters toward smaller cluster luminosities except for a slight shift brightward for the reduced magnitudes of first brightest galaxies in poor clusters. The discontinuity in slope of the ($M_{V,\mathrm{tot}}$, $L_{V,\mathrm{cl}}$)-relation at the junction between poor and rich clusters is not present when $M_{V,\mathrm{tot}}$, which includes the envelope light, is replaced by $M_{V,\mathrm{rd}}$ which does not. The best fit line to the ($M_{V,\mathrm{rd}}$, $L_{V,\mathrm{cl}}$)-relation for all rich and poor clusters gives $L_{V,\mathrm{rd}} \propto L_{\mathrm{cl}}^{0.42}$, about the same as the relation found in the shallow part of the ($M_{V,\mathrm{tot}}$, $L_{V,\mathrm{cl}}$)-relation. Clearly, the steep increase in $M_{V,\mathrm{tot}}$ for $L_{V,\mathrm{cl}} > 2 \times 10^{12}\ L_{\odot}$ is due to the light contribution of the envelopes of the first brightest galaxies in rich clusters. The dispersion about the mean ($M_{V,\mathrm{rd}}$, log $L_{V,\mathrm{cl}}$)-line for all rich and poor clusters is only 0.38 mag. There is no significant difference in the dispersion about the mean line when poor and rich clusters points are considered separately, but there is a systematic shift of the poor cluster points with respect to the rich cluster points. If mean lines are fitted to the poor and rich clusters points separately, the lines are roughly parallel, but on average the reduced magnitudes of first brightest galaxies in poor clusters are about 0.8 mag brighter than the reduced magnitudes of first brightest galaxies in rich clusters for a given cluster luminosity. The dispersion about the mean line for the poor clusters is 0.27 mag, while that for the rich clusters is 0.13 mag, slightly smaller.

In Figure 14 is shown the correlation between $M_{V,\mathrm{tot,E}}$ and the cluster luminosity (filled dots for the poor clusters and crosses for the rich clusters). $M_{V,\mathrm{tot,E}}$ is the total absolute visual magnitude calculated from the reduced absolute magnitude $M_{V,\mathrm{rd}}$ using relation (10) derived for normal ellipticals. Thus $M_{V,\mathrm{tot,E}}$ measures the total luminosity of the galaxy excluding the envelope light. Except for a shift of about 3 mag brightward, the ($M_{V,\mathrm{tot,E}}$, log $L_{V,\mathrm{cl}}$)-relation is basically very similar to the ($M_{V,\mathrm{rd}}$, log $L_{V,\mathrm{cl}}$)-relation. This is not surprising since both $M_{V,\mathrm{rd}}$ and $M_{V,\mathrm{tot,E}}$ exclude the light of the envelope. There are differences of detail: the slope of the ($M_{V,\mathrm{tot,E}}$, log $L_{V,\mathrm{d}}$)-relation is slightly shallower ($L_{V,\mathrm{tot,E}} \propto L_{\mathrm{cl}}^{0.29}$) and the dispersion of all the poor and rich clusters points about the mean line (*dashed line*) is slightly smaller (0.29 mag). Again there is no significant difference in the dispersion about the mean line for all poor and rich clusters when poor and rich clusters are considered separately. A slight systematic shift brightward of 0.6 mag for the poor cluster points with respect to the rich cluster points is again evident. The dispersion about the mean line for poor clusters only is 0.21 mag while that for rich clusters only is 0.11 mag.

Figure 14 also shows (*triangles*) the strong dependence

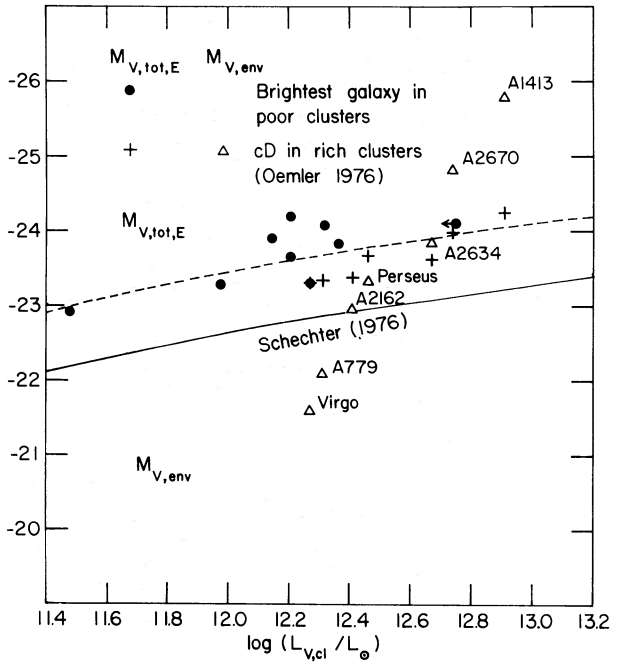


FIG. 14.—The filled dots and the plus signs show the correlation between the absolute visual magnitude $M_{V,\mathrm{tot,E}}$ of the brightest galaxies in poor and rich clusters and the visual luminosity $L_{V,\mathrm{cl}}$ of their clusters. $M_{V,\mathrm{tot,E}}$ is calculated using the observed $M_{V,\mathrm{rd}}$ for the brightest galaxies and the relation derived by Oemler (1976) between $M_{V,\mathrm{rd}}$ and the total magnitude $M_{V,\mathrm{tot}}$ for normal ellipticals (eq. [10]). The solid line is the predicted relation between the absolute visual magnitude of the first brightest galaxy and the visual luminosity of the cluster using Schechter's (1976) luminosity function. The dashed line is the solid line shifted up by 0.8 mag to best fit (by eye) the data.

of the luminosity of the envelope $L_{\mathrm{env}}$ of the first brightest cluster galaxy in rich clusters on cluster luminosity ($L_{\mathrm{env}} \sim L_{\mathrm{cl}}^{2.2}$)(Oemler 1976). $L_{\mathrm{env}}$ is computed as the difference in luminosity between $M_{V,\mathrm{tot}}$ obtained by integrating the measured light profile and $M_{V,\mathrm{tot,E}}$ obtained by using the ($M_{V,\mathrm{rd}}$, $M_{V,\mathrm{tot}}$)-relation for normal ellipticals. The nonexistence of an envelope component in first brightest galaxies in poor clusters implies that the ($L_{\mathrm{env}}$, $L_{\mathrm{cl}}$)-relation steepens even further, becoming nearly vertical for $L_{\mathrm{cl}} \lesssim 1.6 \times 10^{12}\ L_{\odot}$.

Also shown in Figure 14 as a solid line is the relation between the absolute visual magnitude of the first brightest galaxy and the cluster luminosity, *if* first brightest galaxies are randomly drawn from a statistical selection function described by Schechter's (1976) luminosity function of galaxies. It is clear that the absolute magnitudes of the first brightest galaxies (without the envelope luminosity for the ones in rich clusters) are all brighter than the values predicted by Schechter's luminosity function. A shift of the solid line by $\sim 0.5$ mag brightward gives a good fit to the rich cluster points, and a 1.1 mag brightward shift gives a good fit to the poor cluster points, although the best fit to the poor and rich cluster points considered separately is slightly steeper than the solid line. A parallel shift of 0.8 mag brightward brings the solid line to the position of the dashed line which fits all the data points well.

### d) *Nomenclature*

Are first brightest galaxies in poor clusters "true" cD galaxies? Morgan's definition of a cD galaxy, as stated for example in Matthews, Morgan, and Schmidt (1964), is "a supergiant D galaxy" where a D galaxy is one "having an elliptical-like nucleus surrounded by an extensive envelope" (MKW 1975). The first brightest galaxies in rich clusters studied photometrically by Oemler (1976) satisfy both criteria of (1) being a large bright elliptical and (2) possessing an extended envelope; thus they are "true" cD galaxies in the original sense of Morgan. The first brightest galaxies in the poor clusters studied in this paper have all been classified as cD galaxies by MKW and AWM, with the exception of the first brightest galaxy in MKW 9 which is classified as a D2 galaxy. The classification was made after visual inspection by Morgan of the poor clusters on the original negatives of the Sky Survey. Visually, the first brightest galaxies in poor clusters do appear to be bright and to possess a large diffuse envelope. The detailed photographic surface photometry presented in this paper confirms the visual impression of large brightness but does not confirm the presence of an extended envelope as a distinct component from the main body of the elliptical galaxy. In that sense, the studied galaxies are not "true" cD galaxies. In this paper, we refer to these as first brightest galaxies in poor clusters.

## IV. IMPLICATIONS ON FORMATION THEORIES OF FIRST BRIGHTEST GALAXIES IN CLUSTERS

### a) *Results to be Explained*

The previous sections have established clearly two results: (1) First brightest cD galaxies in rich clusters are made up of two components: a main elliptical-like body and a large diffuse envelope. The third component discussed by Dressler (1979) is not evident from the surface photometry alone. In contrast, first brightest galaxies in poor clusters have only one component, the elliptical-like body. (2) The main bodies of first brightest galaxies in both poor and rich clusters are similar to normal elliptical galaxies except that they are brighter and more diffuse (larger core and effective radius, and lower surface brightness). The central bodies of first brightest galaxies in poor clusters are more diffuse than that of cD galaxies in rich clusters (Figs. 11 and 12) and are slightly brighter for a given cluster luminosity (Fig. 14).

Result 1 suggests that first brightest galaxies in clusters are made by at least two distinct physical processes: one process which forms the main elliptical-like body, and one process which accounts for the existence or absence of the envelope component. The first process should be able to explain the trends in brightness, core radius, and surface brightness described in result 2; and the second process should account for the strong dependence of the envelope luminosity on cluster richness.

### b) *Dynamical Friction and the Formation of the Central Body*

We first discuss possible formation processes for the elliptical-like central component. Is the central body created by a statistical process also responsible for normal smaller galaxies and described by the luminosity function of galaxies, or is it created by some special process? Figure 14 and the discussion in § IIIc show that the luminosity of first brightest cluster galaxies without their envelope is in the mean 0.8 mag *brighter* than the luminosity predicted by Schechter's (1976) luminosity function, for a given cluster luminosity. This argues against a statistical formation process. An attractive special creation process for first brightest cluster galaxies has been proposed by Hausman and Ostriker (1978) in which a bright normal galaxy accretes other galaxies, thus growing in luminosity and in core (or effective) radius and decreasing in surface brightness. The theory thus accounts naturally for the properties described in result 2.

With $M_V^* - \langle M_1 \rangle = 1$ mag (where $M_V^*$ corresponds to the characteristic visual luminosity defined in eq. (14) and $M_1$ is the average absolute visual magnitude of first brightest galaxies in *rich* clusters) and $\langle M_1 \rangle - M_{V,\mathrm{tot},E} = 0.5$ mag (Fig. 14), we obtain $M_V^* - M_{V,\mathrm{tot},E} = 1.5$ mag, so that, on average, the first brightest galaxy without its envelope in a rich cluster has a luminosity equal to $4\,L_*$. This is consistent with the merger picture: the time since cluster collapse for a typical Abell cluster is about $4 \times 10^9$ years. The average time between successive mergers, due to orbit decay of cluster galaxies caused by dynamical friction, to form a bright galaxy in a rich cluster, is about $10^9$ years as shown by the numerical simulations of Hausman and Ostriker (1978) so that one would expect approximately four mergers to have occurred. Hoessel (1980) also found, by studying the distribution of surface brightness of first brightest galaxies in his sample of 108 Abell clusters, that about four mergers have occurred to form the brightest galaxy since cluster formation time.

The observation that first brightest galaxies in poor clusters are about 0.6 mag brighter than cD galaxies in rich clusters (without the luminosity of their envelope) and have larger core radii and smaller surface brightness suggests that poor clusters are more dynamically evolved than rich clusters. First brightest galaxies in poor clusters have a luminosity corresponding to about $7L_*$. They have undergone seven mergers of galaxies with characteristic luminosity $L_*$ on the average. It would be interesting to obtain large-scale short-exposure plates of first brightest galaxies in poor clusters to confirm the existence of multiple nuclei in their cores. The faster merging rate in poor clusters compared to that in rich clusters is expected in a galactic cannibalism picture. According to Hausman and Ostriker (1978), massive galaxies collect in the center of a cluster on the relaxation time scale $\tau_R$ per cluster galaxy defined as

$$\tau_R \sim NT_{\mathrm{cr}} \sim NR/\sigma\,, \qquad (16)$$

where $N$ is the number of cluster members, $T_{cr}$ is the cluster crossing-time, $R$ is the cluster characteristic size, and $\sigma$ is the cluster velocity dispersion. The total rate of accretion $A$ onto the central region is proportional to the total number of galaxies in the cluster so that:

$$A \sim N\tau_R{}^{-1} = [R/\sigma]^{-1} = T_{cr}{}^{-1} . \quad (17)$$

The total accretion rate is independent of the number of cluster members and goes inversely as the crossing time. If for a rich cluster $R = 5$ Mpc and $\sigma = 1000$ km s$^{-1}$, and for a poor cluster $R = 1$ Mpc and $\sigma = 500$ km s$^{-1}$ (a value $\sigma = 622$ km s$^{-1}$ is obtained by Stauffer and Spinrad 1980 by measuring redshifts of 11 galaxies in AWM 7 and $\sigma = 397$ km s$^{-1}$ by measuring five galaxies in AWM 5), then the ratio of the accretion rate $A_p$ onto the central galaxy in the poor cluster to the accretion rate $A_r$ in the rich cluster is $A_p/A_r \sim 2.5$, in good agreement with the factor of $\sim 2$ found above for the ratio of luminosities of first brightest galaxies in poor clusters to that in rich clusters. Galactic cannibalism proceeds faster in poor clusters than in rich clusters mainly because poor clusters are more compact: it is easier for the brightest galaxy to grab for its meal.

If dynamical friction occurs faster in poor clusters than in rich clusters, why do some small groups or poor clusters not possess a giant elliptical galaxy? This is because to start the dynamical friction process, an already massive and luminous galaxy, formed by a statistical process (according to a luminosity function such as the one proposed by Schechter 1976) is needed at cluster formation time. In small groups or poor clusters not having a large "seed" galaxy, dynamical friction is inoperative and a giant elliptical galaxy never forms.

Other observational evidence supporting the merger picture follows:

1. The mass-to-light ratio for the brightest galaxies in rich (excluding the envelope) and poor clusters is similar to the mass-to-light ratio derived for normal elliptical galaxies. The cannibal galaxy is expected to have the same mass-to-light ratio as its victims. Only one first brightest galaxy in our sample of poor clusters has a measured velocity dispersion: NGC 1129 in AWM 7, which has an internal velocity dispersion of 272 km s$^{-1}$ (Schwartz *et al.* 1980). This is significantly lower than the core velocity dispersion of 375 km s$^{-1}$ obtained by Dressler (1979) for the cD galaxy in the rich cluster A2029. The global mass-to-light ratio for a galaxy whose light profile is well approximated by de Vaucouleurs's law is given by:

$$\frac{M}{L} = \frac{3\sigma^2 r_e}{0.33GL} \quad (18)$$

(Poveda 1958; Tonry 1980), where $\sigma$ is the measured velocity dispersion, $r_e$ the effective half-light radius (Table 6), and $L$ the total luminosity (Table 5). We obtain a global $M/L_V$ ratio of 13 $M_\odot/L_\odot$ (or $M/L_B = 38\ M_\odot/L_\odot$ with $B-V = 1.17$ from Table 1) for NGC 1129. This is slightly larger but not significantly different from the mean global $M/L_B$ of 27 $M_\odot/L_\odot$ derived by Tonry (1980) for his large sample of normal ellipticals. The highest global $M/L_B$ observed by Tonry (1980) is 64. The derived value of $M/L_V$ of NGC 1129 is nearly equal to that of the inner component Dressler (1979) needed to model the run of light and velocity dispersion as a function of radius in the cD galaxy in A2029, consistent with the idea that the central regions of first brightest galaxies in both poor and rich clusters are formed by the same process. Dressler (1979) also needed two other components: one component composed of luminous material with $M/L_V \sim 35$ in the intermediate regions and one component composed of dark material with $M/L_V > 500$ in the outermost regions. These higher mass-to-light ratio components do not appear to be present in NGC 1129. Presumably they constitute the envelope component which is not present in first brightest galaxies in poor clusters. With a total visual luminosity $L_V = 6.4 \times 10^{11}\ L_\odot$, the total mass of NGC 1129 is $8.4 \times 10^{12}\ M_\odot$. This is comparable to the mass of about $10^{13}\ M_\odot$ derived by Jenner (1974) for the central regions of double nuclei cD galaxies in rich clusters.

2. Giant ellipticals occur in a wide variety of environments—in cD or extreme spiral-poor clusters, but also in spiral-rich poor clusters. Bahcall (1980) found that more than half of the cluster members in most of the MKW, AWM clusters are spiral galaxies, with some having a spiral fraction as large as 0.7. In a merger picture, the cannibal galaxy should not care about the morphological class of its victims.

3. The color-magnitude relation for E and S0 galaxies appears to flatten out at the bright end. This is expected from the cannibalism picture, as the redder cannibal galaxy adopts the bluer color of its victims. Previous studies such as those by Schild and Davis (1979) and Lugger (1979) used the extrapolated magnitudes by Schild and Davis which we have shown to be in error (§ II*d*). We reexamine the data here using our derived $M_{V,\mathrm{Sand}}$, the absolute magnitude within the Sandage (1972*a*) metric diameter of 86 kpc, for the first brightest galaxies in poor clusters (Table 5). The $U-B$ colors as given by Schild and Davis (1979) are plotted as a function of $M_{V,\mathrm{Sand}}$, in Figure 15 for first brightest galaxies in poor clusters (*triangles*). Also plotted are the ellipticals and S0 galaxies in the Virgo (*dots*) and Coma (*crosses*) clusters as given by Sandage (1972*b*). The color and magnitudes have been corrected for galactic obscuration (Sandage 1973) and $K$-effects (Schild and Davis 1971). There is a slight suggestion of flattening of the color-magnitude relation for $M_{V,\mathrm{Sand}} \lesssim -23$ mag. The mean $(U-B)_0$ color for all brightest galaxies in poor clusters (with $-24 \lesssim M_{V,\mathrm{Sand}} \lesssim -22.5$) is $0.52 \pm 0.05$. The $(U-B)_0$, derived by extrapolating the color-magnitude relation for $M_{V,\mathrm{Sand}} \gtrsim -22.5$, at $M_{V,\mathrm{Sand}} = -23.2$ is 0.60.

4. The first brightest galaxies in both poor and rich clusters are usually found near the cluster center, consistent with the buildup of a remnant at the bottom of the cluster's potential well. That they dominate the cluster's potential well is also consistent with the fact that first brightest galaxies in both poor and rich clusters are often associated with strong radio and X-ray sources. M87 and NGC 1275 are well known to be both radio and X-ray

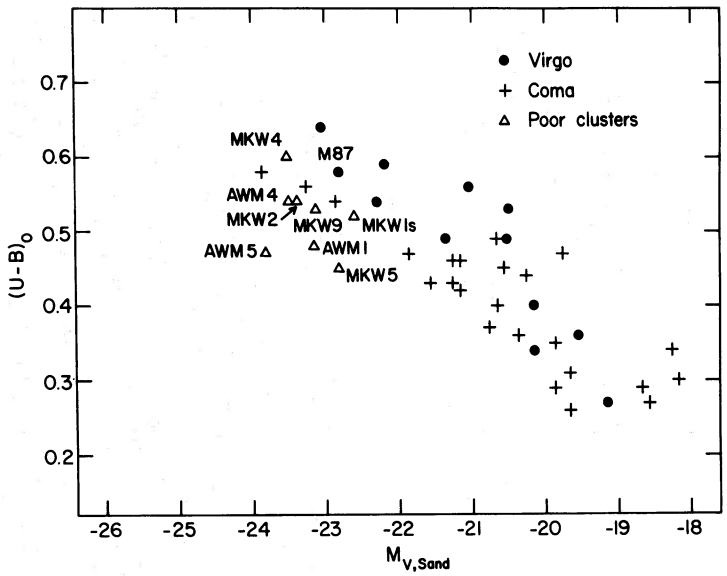


FIG. 15.—The color-magnitude diagram for E and S0 galaxies in the Virgo and Coma clusters (Sandage 1972*b*) and for the brightest galaxies in poor clusters. The colors $(U - B)$ have been corrected to zero redshift and for galactic extinction. $M_{V,\mathrm{Sand}}$ is the absolute visual magnitude within Sandage's (1972*a*) metric diameter of 86 kpc.

sources. There is strong X-ray emission in AWM 7 centered on NGC 1129 (Schwartz *et al.* 1980). The first brightest galaxy in AWM 4 is a strong radio (Burns, White, and Hough 1980) and X-ray (Kriss *et al.* 1980) source.

All these observations are consistent with the merger picture, but do not prove it. We have already noted in § III*b* that the elliptical component of first brightest galaxies in both poor and rich clusters extrapolates very smoothly properties of normal ellipticals. For example, the first brightest galaxies fit well the brightward extension of the $(B_e, \log r_e)$-relation defined by normal ellipticals (Fig. 10). The slope of the best fit to the first brightest galaxies points is only slightly steeper. If normal ellipticals are made by a statistical process (there are serious difficulties with making all ellipticals by merging spiral galaxies—see, for example, Ostriker 1980) and first brightest ellipticals by a merger process, first brightest galaxies (without their envelopes) manage to rearrange their structure so as to look just like normal brighter and more diffuse ellipticals. The similarity between the inner parts of first brightest cluster galaxies with normal ellipticals is also emphasized by the fact that NGC 1129 in AWM 7, which has a measured velocity dispersion of 272 km s$^{-1}$ (Schwartz *et al.* 1980) and an isophotal blue magnitude to the 23d $B$ mag isophotal level $M_{B(0)} = -21.60$, fits almost exactly on the mean $L_B \propto \sigma^4$ relation for normal ellipticals discovered by Faber and Jackson (1976). $M_{B(0)}$ for NGC 1129 has been obtained by integrating the light profile, by using $B - r = 1.47$, and by correcting for galactic absorption (Sandage 1973) and $K$-effects (Schild and Oke 1971). M87, which has $M_{B(0)} = -21.64$ (Kormendy 1977) and a velocity dispersion of 278 km s$^{-1}$ at the edge of its core (Sargent *et al.* 1978), also fits well the mean $L_B \propto \sigma^4$ relation. The similarity of global mass-to-light ratio between NGC 1129, M87, and normal ellipticals is also consistent with the nondependence of $M/L$ on $L$ observed for normal ellipticals by Tonry (1980).

### *c) Galaxy Collisions and Envelope Formation*

We now turn to the discussion of the envelope formation for first brightest galaxies in rich clusters. The nonexistence of an envelope component in first brightest galaxies in poor clusters suggests a sharp cutoff of the envelope formation mechanism when the cluster's richness drops below a certain threshold number. Galaxy collisions provide an attractive way of providing the envelope material. Halo stars are tidally stripped from their parent galaxies in these collisions, move in the general cluster gravitational field, and fall to the bottom of the cluster's potential well. Since the first brightest galaxy created by mergers is also located at the bottom of the potential well (as argued in § IV*b*), the stripped stars form naturally an extended diffuse envelope around the giant elliptical (for a discussion of this scenario, see, for example, Richstone 1976). The average time $T_{\mathrm{coll}}$ between successive collisions of a galaxy with other cluster members is:

$$T_{\mathrm{coll}} = [2^{1/2}\sigma n \pi R_g^{\,2}]^{-1} \sim 10^9 \text{ yr} \times \left[\left(\frac{\sigma_r}{1000 \text{ km s}^{-1}}\right)\left(\frac{n}{1000 \text{ gal Mpc}^{-3}}\right)\left(\frac{R_g}{100 \text{ kpc}}\right)^2\right]^{-1}, \quad (19)$$

where $\sigma$ is the three-dimensional cluster velocity dispersion and $\sigma_r$ is the observed radial velocity dispersion $[\sigma_r = \sigma/(3)^{1/2}]$, $n$ is the galaxy volume density in the

cluster, and $R_g$ is the galaxy radius. For the dense central regions of a rich cluster with $\sigma_r = 1000$ km s$^{-1}$, $n \sim 1000$–10,000 galaxies Mpc$^{-3}$ and $R_g \sim 10$ kpc, the collision time is typically of the order of $10^8$–$10^9$ years, 0.01–0.1 of the Hubble time. For a poor cluster with $\sigma_r = 500$ km s$^{-1}$ and $R_g \sim 10$ kpc, the collision time becomes larger than the Hubble time ($10^{10}$ years) for $n \lesssim 200$ galaxies Mpc$^{-3}$. If cluster galaxies have halos as extended as 50 kpc in radius, the upper limit becomes $n \lesssim 8$ galaxies Mpc$^{-3}$. All the poor clusters included in this study have a galaxy density less than $\sim 10$ galaxies per Mpc$^3$. Galaxies in these poor clusters have not had time to collide with each other. An observational fact which strongly supports this conclusion is the high percentage (as high as 70%) of spirals in the poor clusters (Bahcall 1980). Figure 14 shows that the envelope component is not present when the cluster luminosity drops below $2 \times 10^{12}\ L_\odot$. Using the Schechter (1976) luminosity function (eq. [14]), the cluster total luminosity can be written as:

$$L_{\rm cl} = \int_0^\infty LN(L)dL = \Gamma(1)N^*L^* = N^*L^* . \qquad (20)$$

Using $L_V{}^* = 6.2 \times 10^{10}\ L_\odot$ and $L_{{\rm cl},V} = 2 \times 10^{12}\ L_\odot$, equation (20) gives $N^* = 32$ galaxies. This corresponds to $n^* \sim 8$ galaxies Mpc$^{-3}$ assuming the cluster is spherical and a cluster radius of 1 Mpc, consistent with the rough upper limit for the galaxy density derived from equation (19) with a galaxy radius of 50 kpc. It would be interesting to perform numerical simulations like that of Richstone (1976) to see if the steep dependence of the envelope luminosity on cluster luminosity shown in Figure 14 can be reproduced.

Following is other observational evidence supporting this envelope formation picture: (1) the high $M/L_V$ ratio of the material constituting the envelope is consistent with the idea that it comes from the outer parts of halos of galaxies. Dressler (1979) found he needed two high mass-to-light ratio components (one with $M/L_V \sim 35$ and one with $M/L_V \sim 500$) to account for the light and the velocity dispersion in the envelope of the cD galaxy in A2029. (2) The observation of diffuse light in rich clusters of galaxies is also consistent with the idea of tidal stripping. Thuan and Kormendy (1977) found that the detailed isophotes and the profiles as a function of radius of the diffuse light in the Coma cluster follow the corresponding distributions for galaxies very closely. This should be the case if the diffuse material consisting of loose stripped stars is governed by the same potential as the galaxies. Thuan and Kormendy (1977) also found that the intergalactic diffuse light joined smoothly into the envelope light of the two central galaxies in Coma, suggesting that the diffuse and envelope light have the same origin. The diffuse light is bluer ($B - V = 0.54 \pm 0.18$) than the light from galaxies ($B - V \sim 1.0$), again consistent with the idea that the light comes from stars stripped off the outer parts of the galaxies which are observed to be bluer than the central parts (Strom *et al.* 1977). (3) The rise in the stellar velocity dispersion observed in the outer halo of the cD galaxy in A2029 (Dressler 1979) is also expected in such a picture. As debris from galaxy-galaxy encounters, the velocity dispersion of the stars in the cD envelope ought to reflect that of the galaxies within the cluster ($\sim 1000$ km s$^{-1}$) rather than the internal galaxy velocity dispersion of $\sim 350$ km s$^{-1}$. We thus expect the velocity dispersion in the outer parts of first brightest galaxies in poor clusters to *decrease* (or remain constant) *rather than increase*, because of the lack of an envelope.

Finally we note that Kormendy (1977) has proposed another mechanism which can cause excess light above the de Vaucouleurs $r^{1/4}$ law in normal ellipticals. He interprets the excess light in these lower luminosity ellipticals as due to tidal effects from neighbor galaxies. In view of the fact that most of the first brightest galaxies in poor clusters do have companion galaxies and yet do not deviate from de Vaucouleurs's law (Fig. 1), tidal distension does not seem to be the major cause for the large extended envelopes seen in cD galaxies in rich clusters. Tidal effects are not important in this context because first brightest galaxies in poor and rich clusters are so much more massive than their neighbor galaxies.

## V. SUMMARY

We have presented in this paper detailed photographic surface photometry of nine first brightest galaxies in poor clusters suspected to be cD galaxies by Morgan, Kayser, and White (1975) and Albert, White, and Morgan (1977). The surface photometry is put on an absolute scale using multiaperture photoelectric photometry in the Thuan and Gunn (1976) system.

Oemler (1976) and de Vaucouleurs (1948) laws are fitted to the profiles to derive structural parameters. Structural properties of first brightest galaxies in poor clusters are compared with that of the cD galaxies in rich clusters studied by Oemler (1976) and that of normal ellipticals studied by Kormendy (1977). The following is found: (1) Profiles of first brightest galaxies are well fitted by an $r^{1/4}$ law over a range of more than 9 mag and down to the faintest light levels observed (Fig. 1). In contrast, the profiles of first brightest galaxies in rich clusters exhibit a systematic excess of light above the $r^{1/4}$ law in the outer parts (Fig. 7). Because of the lack of an envelope component, first brightest galaxies in poor clusters are not "true" cD galaxies in the Morgan sense. (2) Structural parameters characterizing only the central part of first brightest galaxies in poor and rich clusters and excluding the envelope component in the case of rich clusters extend smoothly properties exhibited by normal ellipticals such as, for example, the ($B_e$, log $r_e$)-relation. The main bodies of first brightest galaxies in both poor and rich clusters are similar to normal ellipticals except that they are brighter and more diffuse, i.e., they have larger cores and effective radii and lower surface brightness. The central bodies of first brightest galaxies in poor clusters are more diffuse than that of cD galaxies in rich clusters (Figs. 11 and 12) and are about 0.6 mag brighter for a given cluster luminosity. (3) The meager dynamical data on first brightest galaxies in poor and rich clusters such as

internal velocity dispersion data also suggest that their central parts are similar to normal ellipticals. The central parts have comparable global mass-to-light ratio ($M/L_V \sim 13$) and fit well on the $L \propto \sigma^4$ relation defined by normal ellipticals. (4) The central parts of cD galaxies in rich clusters are $\sim 0.5$ mag brighter and that of first brightest galaxies in poor clusters are $\sim 1.1$ mag brighter than what would be predicted from Schechter's (1976) luminosity function, given their cluster luminosities (Fig. 14).

These observations are consistent with the idea that the central body of first brightest galaxies in both poor and rich clusters is made up by mergers of smaller galaxies. On the average, a cD galaxy in a rich cluster would have undergone four mergers of galaxies with characteristic luminosity $L_*$ since cluster formation, while a first brightest galaxy in a poor cluster would have undergone seven mergers. The faster merging rate in poor clusters is mainly due to their compactness. The observations suggest that the envelopes of cD galaxies in rich clusters are made up of stellar tidal debris resulting from galaxy-galaxy encounters. The absence of an envelope component in first brightest galaxies in poor clusters is due to a collision time larger than the Hubble time in these clusters.

T. X. T. thanks the director of Palomar Observatory for generous allotments of telescope time and acknowledges partial financial support from NASA grant NAG5-61 and the Research Corporation. He also thanks Dr. Jean Audouze for his warm hospitality at the Institut d'Astrophysique of the Centre National de la Recherche Scientifique in Paris where part of this work was done.

## REFERENCES


Aaronson, M., Mould, J., Huchra, J., Sullivan, W., Schommer, R., and Bothun, G. 1980, *Ap. J.*, **239**, 12.
Albert, C. E., White, R. A., and Morgan, W. W. 1977, *Ap. J.*, **211**, 309 (AWM).
Bahcall, N. A. 1980, *Ap. J.* (*Letters*), **238**, L117.
Burns, J. O., White, R. A., and Hough, D. H. 1981, *A.J.*, **86**, 1.
Carter, D., and Dixon, K. L. 1978, *A.J.*, **83**, 574.
de Vaucouleurs, G. 1948, *Ann. d'Ap.*, **11**, 247.
de Vaucouleurs, G., de Vaucouleurs, A., and Corwin, G. H., Jr. 1976, *Second Reference Catalogue of Bright Galaxies* (Austin: University of Texas Press).
Dressler, A. 1979, *Ap. J.*, **231**, 659.
Faber, S. M., and Jackson, R. E. 1976, *Ap. J.*, **204**, 668.
Hausman, M. A., and Ostriker, J. P. 1978, *Ap. J.*, **224**, 320.
Hoessel, J. G. 1980, *Ap. J.*, **241**, 493.
Hoessel, J. G., Gunn, J. E., and Thuan, T. X. 1980, *Ap. J.*, **241**, 486.
Holmberg, E. 1958, *Medd. Lunds. Astr. Obs.*, Vol. **2**, No. 136.
Huchra, J. P. 1976, *A.J.*, **81**, 592.
Jenner, D. C. 1974, *Ap. J.*, **191**, 55.
Jensen, E. B., and Thuan, T. X. 1981, *Ap. J.*, submitted.
King, I. 1966, *A.J.*, **71**, 64.
Kormendy, J. 1977, *Ap. J.*, **218**, 333.
———. 1980, in *Proceedings of ESO Workshop on Two-Dimensional Photometry*, ed. P. Crane and K. Kjär (Geneva: ESO), p. 191.
Kriss, G. A., Canizares, C. R., McClintock, J. E., and Feigelson, E. D. 1980, *Ap. J.* (*Letters*), **235**, L61.
Lugger, P. M. 1979, *A.J.*, **84**, 1677.
Matthews, T. A., Morgan, W. W., and Schmidt, M. 1964, *Ap. J.*, **140**, 35.
Mendoza, E. E. 1967, *Bol. Obs. Tonantzintla y Tacubaya*, **4**, 149.
Morgan, W. W., Kayser, S., and White, R. A. 1975, *Ap. J.*, **199**, 545 (MKW).
Noonan, T. W. 1973, *A.J.*, **78**, 26.
Oemler, A. 1976, *Ap. J.*, **209**, 693.
Ostriker, J. P. 1980, *Comments Ap.*, **8**, 177.
Poveda, A. 1958, *Bol. Obs. Tonantzintla y Tacubaya*, **17**, 3.
Richstone, D. O. 1976, *Ap. J.*, **204**, 642.
Sandage, A. 1972*a*, *Ap. J.*, **173**, 485.
———. 1972*b*, *Ap. J.*, **176**, 21.
———. 1973, *Ap. J.*, **183**, 711.
Sandage, A., Kristian, J., and Westphal, J. A. 1976, *Ap. J.*, **205**, 688.
Sargent, W. L. W., Young, P. J., Boksenberg, A., Shortridge, K., Lynds, C. R., and Hartwick, F. D. A. 1978, *Ap. J.*, **221**, 731.
Schechter, P. 1976, *Ap. J.*, **203**, 297.
Schild, R., and Davis, M. 1979, *A.J.*, **84**, 311.
Schild, R., and Oke, J. B. 1971, *Ap. J.*, **169**, 209.
Schwartz, D. A., *et al.* 1980, *Ap. J.* (*Letters*), **238**, L53.
Stauffer, J., and Spinrad, H. 1978, *Pub. A.S.P.*, **90**, 20.
———. 1980, *Ap. J.*, **235**, 347.
Strom, K. M., and Strom, S. E. 1978*a*, *A.J.*, **83**, 73.
———. 1978*b*, *A.J.*, **83**, 732.
Strom, K. M., Strom, S. E., Jensen, E. B., Moller, J., Thompson, L. A., and Thuan, T. X. 1977, *Ap. J.*, **212**, 335.
Thomas, J. C., and Batchelor, D. 1978, *A.J.*, **83**, 1160.
Thuan, T. X. 1981, in preparation.
Thuan, T. X., and Gunn, J. E. 1976, *Pub. A.S.P.*, **88**, 543.
Thuan, T. X., and Kormendy, J. 1977, *Pub. A.S.P.*, **89**, 466.
Thuan, T. X., and Romanishin, W. 1979, in *Photometry, Kinematics, and Dynamics of Galaxies*, ed. D. S. Evans (Austin: University of Texas Press), p. 63.
Tonry, J. 1980, Ph. D. thesis, Harvard University.
Turner, E. L., and Gott, J. R., III. 1976, *Ap. J.*, **209**, 6.
van den Bergh, S. 1978, *Pub. A.S.P.*, **89**, 746.
Zwicky, F., Herzog, E., Wild, P., Karpowicz, M., and Kowal, C. 1961–1968, *Catalogue of Galaxies and Clusters of Galaxies* (Pasadena: California Institute of Technology).


WILLIAM ROMANISHIN: Department of Astronomy, University of California, Math-Sciences Building, Los Angeles, CA 90024

TRINH X. THUAN: Department of Astronomy, University of Virginia, P.O. Box 3818, University Station, Charlottesville, VA 22903